

RESEARCH ARTICLE

Cyclin-dependent kinase 1-mediated AMPK phosphorylation regulates chromosome alignment and mitotic progression

Seth Stauffer^{1,2}, Yongji Zeng^{1,2}, Montserrat Santos³, Jiuli Zhou^{1,2}, Yuanhong Chen¹ and Jixin Dong^{1,*}

ABSTRACT

AMP-activated protein kinase (AMPK), a heterotrimeric serine/threonine kinase and cellular metabolic sensor, has been found to regulate cell cycle checkpoints in cancer cells in response to energetic stress, to harmonize proliferation with energy availability. Despite AMPK's emergent association with the cell cycle, it still has not been fully delineated how AMPK is regulated by upstream signaling pathways during mitosis. We report, for the first time, direct CDK1 phosphorylation of both the catalytic α 1 and α 2 subunits, as well as the β 1 regulatory subunit, of AMPK in mitosis. We found that AMPK-knockout U2OS osteosarcoma cells have reduced mitotic indexes and that CDK1 phosphorylation-null AMPK is unable to rescue the phenotype, demonstrating a role for CDK1 regulation of mitotic entry through AMPK. Our results also denote a vital role for AMPK in promoting proper chromosomal alignment, as loss of AMPK activity leads to misaligned chromosomes and concomitant metaphase delay. Importantly, AMPK expression and activity was found to be critical for paclitaxel chemosensitivity in breast cancer cells and positively correlated with relapse-free survival in systemically treated breast cancer patients.

KEY WORDS: AMPK, Mitotic phosphorylation, CDK1, Taxol sensitivity

INTRODUCTION

Mitosis is a dynamic and vitally important process for separating identical copies of genomic material into two daughter cells. It is thought that failure in the mitotic processes can lead to tumor initiation (Bakhoun and Swanton, 2014; Nowak et al., 2002; Pino and Chung, 2010). One of the hallmarks of cancer is mitotic defects, frequently seen as flaws in chromosomal adhesion, spindle attachment, chromosomal segregation, cytokinesis and centrosomal duplication (Schvartzman et al., 2010; Kops et al., 2004; Rao and Yamada, 2013). Another important path to cellular transformation is a change in the fidelity of mitotic checkpoints. Mutations or aberrations in the regulation of cell cycle checkpoints often result in what is known as mitotic cell death (MCD) (Kops et al., 2005) or lead to cancer (Reiter et al., 2006; Shichiri et al., 2002), indicating the importance of these checkpoints.

Dramatic changes to major organelles and cellular organization happen swiftly during this relatively short period of the cell cycle.

This window is considered the most vulnerable period of the cell cycle and, subsequently, has become the target of multiple anti-cancer drugs. Many aim to activate the spindle assembly checkpoint (SAC) or to target components of the anaphase-promoting complex (APC), leading to prolonged mitotic arrest and eventual activation of pathways promoting MCD (Manchado et al., 2012). Thus, identifying additional molecular regulation in mitosis may lead to the identification of potentially druggable targets and the development of novel chemotherapeutics for combatting cancer.

AMPK is a heterotrimeric serine/threonine kinase consisting of a catalytic α subunit and two regulatory β and γ subunits. Known to be phosphorylated by kinases LKB1 (also known as STK11) and the CAMKK protein family, AMPK regulates cellular energy homeostasis and harmonizes proliferation with energy availability. Additionally, proliferation is adjusted through metabolic signals that have been shown previously to be coupled to cell cycle progression (Mihaylova and Shaw, 2011). Of importance, AMPK has been found to sit in the center of a signaling network involving bona fide tumor suppressors (Zadra et al., 2015) and to be associated with cell cycle checkpoints, as AMPK-null *Drosophila* cells have mitotic defects (Lee et al., 2007). AMPK has also been shown to be activated during mitosis, with increased p-T172 phosphorylation seen during mitosis (Vazquez-Martin et al., 2009, 2012; Thaiparambil et al., 2012; Mao et al., 2013; Lee et al., 2015; Doménech et al., 2015). Likewise, a screen of AMPK substrates revealed multiple downstream mitotic proteins as targets of its kinase activity (Banko et al., 2011). A chemical genetic screen of downstream AMPK substrates in human cells identified several that were involved in mitosis, including protein phosphatase 1 regulatory subunit 12A and 12C (PPP1R12A and PPP1R12C), cell division cycle protein 27 (CDC27), and p21-activated protein kinase (PAK2) (Banko et al., 2011). AMPK phosphorylation of PPP1R12C blocks its inhibition of myosin regulatory light chain proteins (MRLCs), which are regulators of cytokinesis (Ito et al., 2004). CDC27 is a member of the APC connecting AMPK to the spindle checkpoint during metaphase (Peters, 2006), and AMPK activation of PAK2 leads to phosphorylation of MRLCs and mitotic progression (Tuazon and Traugh, 1984). MRLCs have also been shown to be phosphorylated directly by AMPK at their regulatory site *in vitro* and *in vivo*, both in *Drosophila* and mammals (Mirouse et al., 2007). AMPK has been connected to mitosis in other studies as well. AMPK-null *Drosophila* embryos display severe abnormalities in cytoskeletal apical-basal polarity, as well as defective mitotic divisions that lead to polyploidy (Lee et al., 2007). Loss of AMPK activity, through either inhibition of AMPK in cancer cells (Sanli et al., 2010) or with full AMPK knockout (KO) in mouse embryonic fibroblasts (MEFs) (Sanli et al., 2012), is enough to weaken the cell cycle arrest at G₂/M caused by ionizing radiation. Interestingly, due to the important role microtubules play in mitotic cell division, inhibition of AMPK has been shown to impair microtubule stabilization through loss of phosphoregulation of the microtubule

¹Eppley Institute for Research in Cancer & Allied Diseases, Fred & Pamela Buffett Cancer Center, University of Nebraska Medical Center, Omaha, NE 68198, USA.

²Department of Pathology and Microbiology, University of Nebraska Medical Center, Omaha, NE 68198, USA. ³Department of Chemistry and Department of Biology, College of Saint Mary, Omaha, NE 68106, USA.

*Author for correspondence (dongj@unmc.edu)

DOI: 10.1242/jcs.236000

plus-end protein CLIP-170 (also known as CLIP1) (Nakano et al., 2010). There is evidence that CLIP-170 itself mediates paclitaxel sensitivity in breast cancer cells through its ability to strengthen microtubule assembly promoted by paclitaxel (Sun et al., 2012). AMPK is also active in the mitotic regulation of neural stem cells. Abolishing normal AMPK activity in the developing mouse brain leads to flawed mitosis in neural progenitor cells and abnormal brain development (Dasgupta and Milbrandt, 2009). Recently, it has been discovered that AMPK and its ortholog Snf1 in *S. cerevisiae* are required for proper metaphase spindle alignment (Thaiparambil et al., 2012; Tripodi et al., 2018). Together, these studies point to a role for AMPK outside of its canonical signaling network, acting as a master regulator not only of cellular metabolism, but also cell cycle progression. Despite AMPK's connection to mitosis, how AMPK is regulated during mitotic progression remains unclear. In this report, we identify a novel layer of regulation involving CDK1-mediated phosphorylation for AMPK.

RESULTS

AMPK is phosphorylated during anti-tubulin drug-induced mitotic arrest

To examine the phosphorylation status of the AMPK subunits, we used PhosTag gel electrophoresis which selectively separates phosphorylated from unphosphorylated proteins through specific binding of phosphate ions (see Zhang et al., 2015; Stauffer et al., 2017). The mobility shifts of AMPK α 1, AMPK α 2 and AMPK β 1 (also known as PRKAA1, PRKAA2 and PRKAB1, respectively) were seen to be increased during mitotic arrest induced by anti-mitotic drugs (Fig. 1A), suggesting that AMPK is phosphorylated during mitotic arrest. The mobility of AMPK β 2, AMPK γ 1, AMPK γ 2 and AMPK γ 3 (also known as PRKAB2, PRKAG1, PRKAG2 and PRKAG3, respectively) were not altered under these conditions (Fig. 1A). We found that the phosphorylation levels of AMPK α 1 and AMPK α 2 at the main T172 activation site and AMPK β 1 at S108 and S182 were not changed under these conditions. This suggests that the mobility shift of AMPK was not likely due to phosphorylation at T172 or S108/S182 respectively and indicates the possibility of novel post-translational modification sites (Fig. 1B). Treatment of arrested cells with λ -phosphatase completely reversed the mobility shift of AMPK α and AMPK β 1 (Fig. 1C), indicating that the mobility shifts of AMPK subunits during mitosis were due to phosphorylation events. In order to determine which upstream kinases could be phosphorylating AMPK, we took cells that were cultured overnight with taxol and then treated for 2 h with various kinase inhibitors. Interestingly, only the CDK1 inhibitors RO-3306 and purvalanol A were able to block the mobility shift for AMPK α (Fig. 1D) and AMPK β 1 (Fig. 1E), signifying that possibly CDK1 is phosphorylating AMPK directly or may be acting further upstream. Taken together, these data suggest that mitotic arrest-induced AMPK phosphorylation is CDK1 dependent.

CDK1 phosphorylates AMPK *in vitro*

In vitro kinase assays were performed to determine whether CDK1 can directly phosphorylate AMPK α , with GST-tagged AMPK α as substrate. Lysates of taxol-treated mitotic HeLa cells strongly phosphorylated AMPK α , and RO-3306 inhibition of CDK1 significantly reduced phosphorylation of GST-AMPK α (Fig. 2A). Database analysis revealed multiple sites in AMPK α 1, AMPK α 2 and AMPK β 1 as mitotic phosphorylation sites from large-scale phosphoproteomic studies (Daub et al., 2008; Dulla et al., 2010; Dephoure et al., 2008). Scanning the amino acid sequences of the AMPK α 1 and AMPK α 2 subunits for CDK1 consensus motifs

identified two potential phosphorylated sites: T382 and T490 on AMPK α 1 and S377 and T485 on AMPK α 2, which are located in the AMPK α ST-stretch (Fig. 2B). Cross-species alignment of AMPK α (Fig. 2B) and of AMPK β 1 (data not shown) subunits show a conservation of the regions flanking these sites, indicating that, possibly, these phosphorylation sites have functional roles. Interestingly, T490 was recently found to be an inhibitory phosphorylation site, regulated by GSK3, which is involved in metabolic flexibility (Suzuki et al., 2013). We next examined whether mutating these sites to alanine would affect CDK1 phosphorylation of AMPK α 2. GST-AMPK α 2-mutants with S377A and T485A combined (AMPK α 2-2A) completely blocked 32 P labeling on AMPK α by active CDK1–cyclin B1 complex when compared with wild-type (WT) GST-AMPK α 2 (Fig. 2C). After identifying these sites, we generated a phospho-specific antibody for detecting p-S377 and utilized the anti-p-T490 AMPK α 1 antibody (Suzuki et al., 2013) for detecting p-T485 of AMPK α 2. As expected, GST-AMPK α 2-WT incubated with activated CDK1–cyclin B1 displayed high levels of phosphorylation detected with anti-p-S377 and anti-p-T485 antibodies, whereas mutating the two sites to alanine completely abrogated the phospho-signal, confirming the specificity of the phospho-antibodies (Fig. 2D). We also examined whether PLK1 is able to phosphorylate AMPK, as one study described regulation of AMPK by PLK1 at T172 during mitosis (Vazquez-Martin et al., 2011). We found that PLK1 fails to phosphorylate either of our mitotic sites and both CDK1 and PLK1 were unable to phosphorylate T172 directly (Fig. 2D).

Similarly, *in vitro* kinase assays were performed to determine whether CDK1 can directly phosphorylate AMPK β 1, with GST-tagged AMPK β 1 as substrate. Lysates of mitotically arrested cells robustly phosphorylated AMPK β 1, with RO-3306 inhibition of CDK1 significantly reducing phosphorylation of GST-AMPK β 1 (Fig. 2E). Next, the phosphorylation sites of T19 and S40 were identified on AMPK β 1 that matched the CDK1 consensus motif and likewise were hits in large-scale phosphoproteomic studies (Daub et al., 2008; Dulla et al., 2010; Dephoure et al., 2008). Interestingly, in line with our observations in Fig. 1A, indicating that AMPK β 1, but not AMPK β 2, is phosphorylated, both T19 and S40 do not exist in AMPK β 2. *In vitro* kinase assays with activated CDK1–cyclin B1 complex displayed clear phosphorylation of GST-AMPK β 1 WT. Interestingly, the AMPK β 1 T19A, and combined T19A and S40A (2A) mutations blocked all 32 P incorporation at both T19 and S40, possibly indicating that lack of T19 phosphorylation precludes S40 phosphorylation, but not vice versa (Fig. 2F). Next, we generated a phospho-specific antibody towards pT19 and found that both AMPK β 1 WT and S40A were clearly phosphorylated at T19, while the T19A and 2A mutants were not (Fig. 2G), once again showing that T19A could be considered identical to 2A.

AMPK is phosphorylated in cells in a CDK1-dependent manner

After confirming AMPK phosphorylation by CDK1 *in vitro*, we next examined this phosphorylation in cells. Immunoprecipitation of endogenous AMPK α 2 from HeLa cells treated with nocodazole or with nocodazole plus RO-3306 showed an increase and a loss of S377 phosphorylation, respectively (Fig. 3A). Overexpressed FLAG-AMPK α 2-WT, -S377A and -T485A constructs transfected into 293T cells treated with or without nocodazole, when FLAG-immunoprecipitated, revealed increased S377 phosphorylation for AMPK α 2-WT under nocodazole treatment and, unsurprisingly, a complete loss in the S377A mutant. Of note, mutating T485 to alanine does not perturb the phosphorylation at S377 (Fig. 3B). These

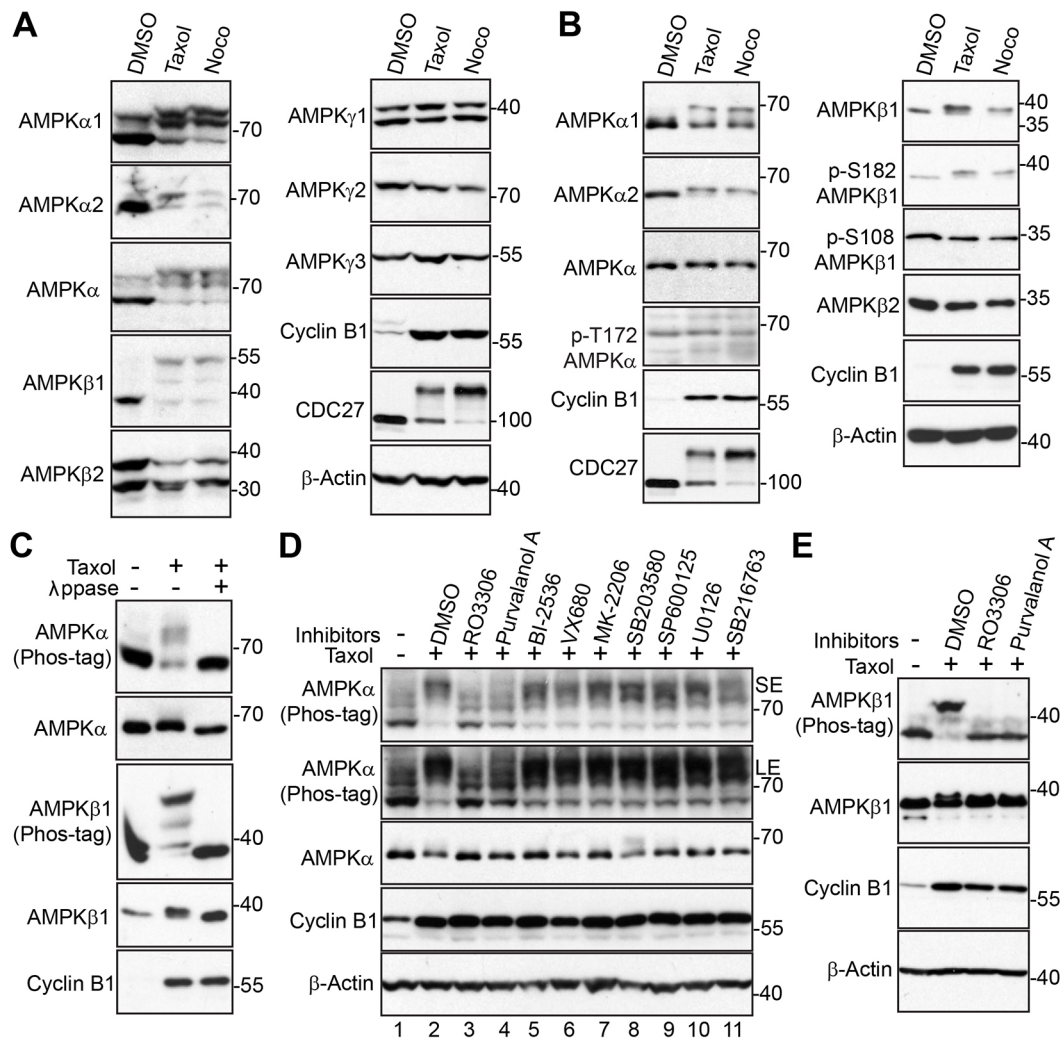


Fig. 1. Phosphorylation of AMPK subunits by CDK1 during mitotic arrest. (A) HeLa cells were treated with DMSO, taxol (100 nM for 16 h) or nocodazole (100 ng/ml for 16 h). Total cell lysates were probed on Phos-tag SDS polyacrylamide gels with antibodies against the indicated proteins. Cyclin B1, CDC27 and β -actin blots were from regular gels. (B) Total cell lysates from the same experiment as in A were electrophoresed on regular SDS polyacrylamide gels and probed with antibodies against the indicated proteins. (C) HeLa cells were treated with taxol as indicated and cell lysates were further treated with (+) or without (–) λ -phosphatase (λ ppase). Total cell lysates were probed with antibodies against the indicated proteins. (D) HeLa cells were treated with taxol, with or without various kinase inhibitors as indicated. RO3306 (5 μ M), purvalanol A (10 μ M), BI-2536 (100 nM), VX680 (2 μ M), MK-2206 (10 μ M), SB203580 (10 μ M), SP600125 (20 μ M), U0126 (20 μ M) and SB216763 (10 μ M) were used. Inhibitors were added 1 h before harvesting the cells (with MG132 to prevent cyclin B degradation and subsequent mitotic exit). Total cell lysates were electrophoresed on regular and Phos-tag SDS polyacrylamide gels and probed with antibodies against the indicated proteins. (E) HeLa cells were treated with taxol, with or without the CDK1 inhibitors as indicated. RO3306 (5 μ M), purvalanol A (10 μ M). Total cell lysates were electrophoresed on regular and Phos-tag SDS polyacrylamide gels and probed with antibodies against the indicated proteins.

data indicate that AMPK α is phosphorylated at S377 in cells during nocodazole-induced mitotic arrest in a CDK1-dependent manner. Next, to determine whether the β 1 subunit was also phosphorylated in cells, we performed FLAG-immunoprecipitation of WT and T19A mutant AMPK β 1 from nocodazole-arrested cell lysates and probed them using the phospho-specific anti-AMPK β 1 T19 antibody. Indeed, the phosphorylation signal was potentially increased for AMPK β 1-WT in cells arrested in mitosis, but completely absent in the T19A mutant (Fig. 3C). Subsequently, we transfected HA-AMPK α 1-WT and HA-AMPK α 1-2A into 293T cells and immunoprecipitated HA-AMPK α 1 from cells treated with either DMSO, taxol or nocodazole. The phosphorylation of HA-AMPK α 1-WT was found to be increased under taxol and nocodazole arrest, but entirely lost in the HA-AMPK α 1-2A mutant (Fig. 3D). To further confirm this as a CDK1-mediated phosphorylation in cells, we immunoprecipitated HA-AMPK α 1-WT and HA-AMPK α 1-2A

from cells treated with nocodazole or with nocodazole plus RO3306. We detected an increase of T490 phosphorylation with nocodazole treatment that could be largely abolished with the CDK1 inhibitor, RO3306, as well as a complete block of this phosphorylation in the HA-AMPK α 1-2A mutant (Fig. 3E). Furthermore, enhanced expression of constitutively active cyclin B1 promoted AMPK phosphorylation at T490 (α 1), S377 (α 2) and T19 (β 1) (Fig. 3F,G).

Next, we wanted to ascertain whether any of the mitotic phosphorylations were essential for AMPK subunit molecular interaction. For this, we co-expressed Myc-AMPK γ 1 with either WT or 2A HA-AMPK α 1 and WT or T19A FLAG-AMPK β 1 in 293T cells, then treated with or without nocodazole and co-immunoprecipitated by pulling down HA-AMPK α 1. Our results showed that neither of the phospho-null mutations in AMPK α 1 or AMPK β 1 had any deleterious effect on subunit interaction (Fig. 3H).

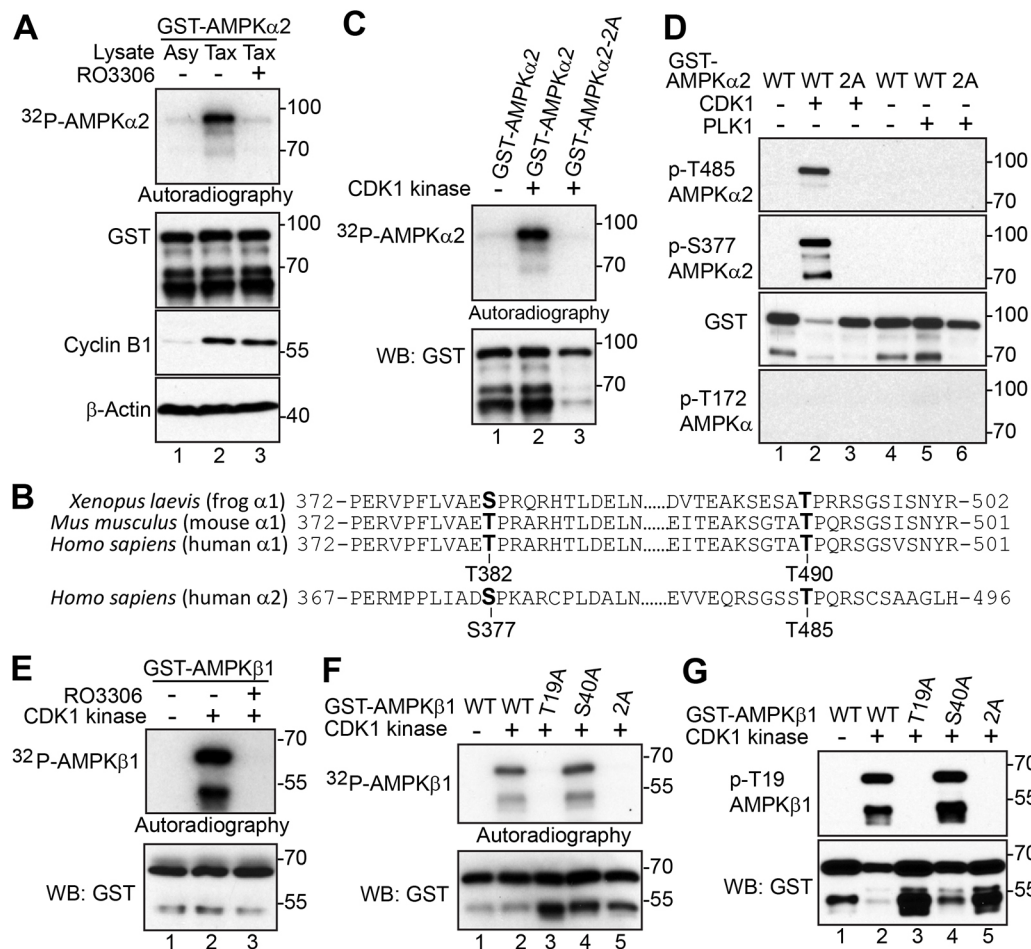


Fig. 2. CDK1 phosphorylates AMPK subunits *in vitro*. (A) *In vitro* 32 P kinase assays with lysates of mitotically arrested HeLa cells and recombinant GST-AMPK α 2. RO3306 (5 μ M) was used to inhibit CDK1 kinase activity. (B) Conservation of AMPK mitotic phosphorylation sites. (C) *In vitro* 32 P kinase assays with purified CDK1-cyclin B1 complex and recombinant GST-AMPK α 2 or GST-AMPK α 2-2A (S377A/T485A). (D) *In vitro* kinase assays with purified CDK1-cyclin B1 complex or activated PLK1 and recombinant GST-AMPK α 2 or GST-AMPK α 2-2A and probed with phospho-specific antibodies. (E) *In vitro* 32 P kinase assays with purified CDK1-cyclin B1 complex and recombinant GST-AMPK β 1. RO3306 (5 μ M) was used to inhibit CDK1 kinase activity. (F) *In vitro* 32 P kinase assays with purified CDK1-cyclin B1 complex to phosphorylate recombinant GST-AMPK β 1, GST-AMPK β 1-T19A, GST-AMPK β 1-S40A or GST-AMPK β 1-2A. (G) *In vitro* kinase assays using purified CDK1-cyclin B1 complex to phosphorylate recombinant GST-AMPK β 1, GST-AMPK β 1-T19A, GST-AMPK β 1-S40A or GST-AMPK β 1-2A (T19A/S40A) and probed with phospho-specific antibody.

AMPK has several autophosphorylation sites (Olgenschlaeger et al., 2015; Woods et al., 2003; Mitchelhill et al., 1997), so we wanted to determine whether AMPK mitotic phosphorylation was due to autophosphorylation or whether AMPK kinase activity was required via feedback mechanisms for the S377 mitotic phosphorylation to occur. To do this, we transfected WT and kinase-dead (K45R) HA-AMPK α 2 in 293T cells, which were treated with or without nocodazole, and then examined the levels of p-S377 (Fig. 3I). We found that there was no difference between the WT and K45R mutant for AMPK α 2 S377 mitotic phosphorylation, indicating that this is not an autophosphorylation site and that AMPK kinase activity is not a precondition for S377 mitotic phosphorylation. Overall, these data provide an argument that CDK1 phosphorylates multiple AMPK subunits in cells during mitosis.

We collected samples from a double thymidine block-and-release and determined the phospho-status of AMPK. p-S377 signal was increased when cells enter into mitosis (8–10 h after being released from double thymidine block) (Fig. 3J). Very weak signals were detected in interphase or cytokinesis cells under freely cycling conditions (Fig. 3K, yellow arrows). The phospho-signal was significantly increased in cells in mitosis (Fig. 3K, white arrows).

These observations indicates that phosphorylation of AMPK S377 occurs during normal mitosis.

AMPK regulates mitotic progression

After we had ascertained that AMPK mitotic phosphorylation is mediated by CDK1, we wanted to explore AMPK's possible role in regulating mitotic processes through gene knockout phenotypic analysis. We generated an AMPK α 1/ α 2 double knockout (AMPK α -KO) and as well as an AMPK β 1 knockout (AMPK β 1-KO) in U2OS cells using a CRISPR-Cas9 approach. In the AMPK α -KO cells, not only was AMPK α 1 and AMPK α 2 expression completely absent, but also both the AMPK β subunit protein levels were severely diminished, indicating a need for AMPK α subunits for stability of the other complex members (Fig. 4A). In the AMPK β 1-KO cell line, aside from AMPK β 1 protein expression being completely lost, AMPK β 2 and AMPK α 1/ α 2 expression remained unchanged (Fig. 4B). Next, we took WT and AMPK α -KO U2OS cells, arrested them at metaphase with nocodazole, and then released the rounded-up mitotic cells in fresh media. Upon release, we harvested cells at the indicated time points and probed for cyclin B1, CDC25C and CDC27 to detect the rate of mitotic exit of each cell line. No

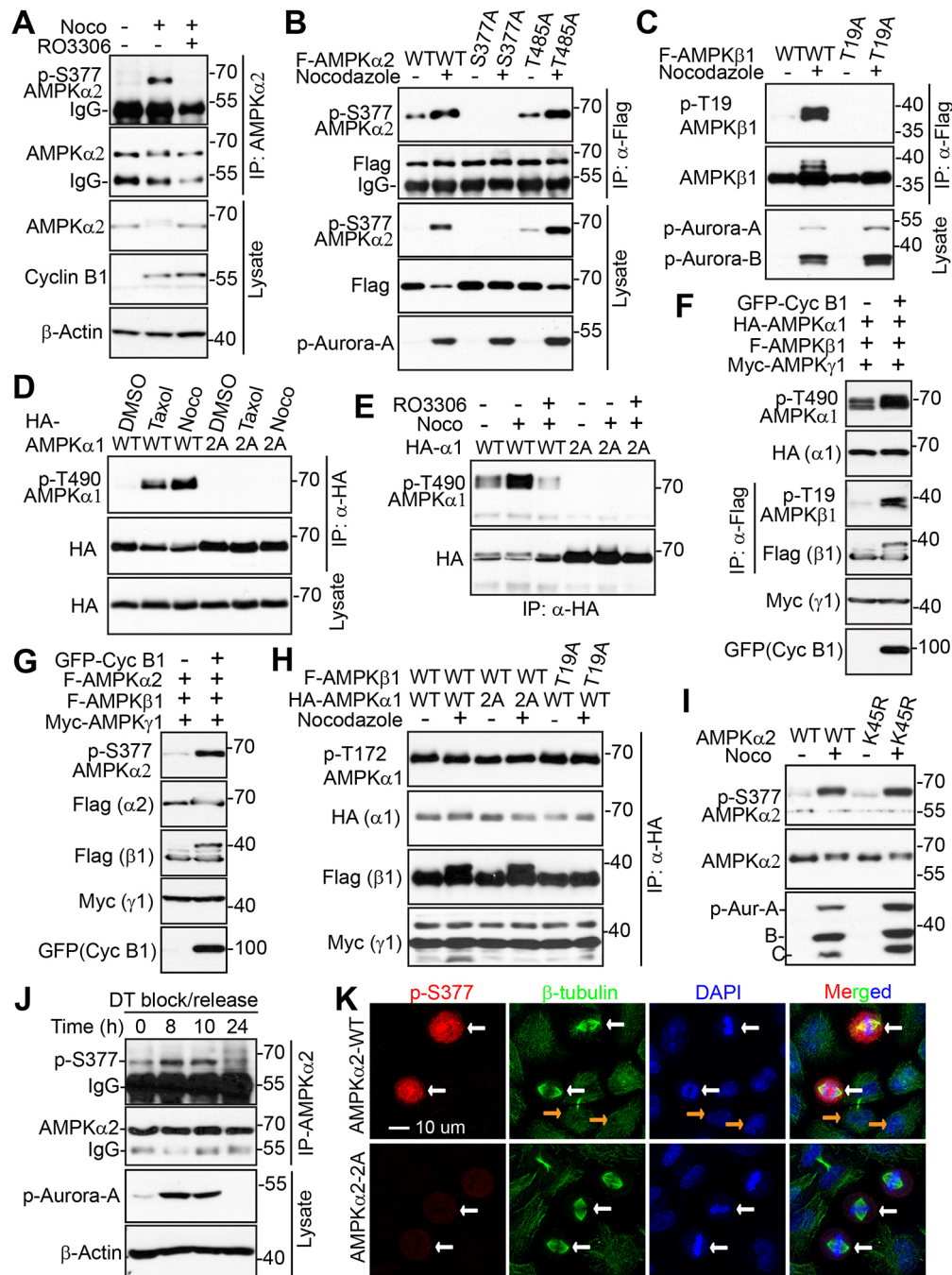


Fig. 3. CDK1 phosphorylates AMPK subunits in cells. (A) Endogenous AMPKα2 immunoprecipitation in HeLa cells treated with nocodazole (16 h) or nocodazole (16 h) with RO3306 and MG132 (1 h) and probed with anti-p-S377 antibody. (B) HEK293T cells transfected with FLAG-AMPKα2-WT, FLAG-AMPKα2-S377A or FLAG-AMPKα2-T485A and treated with taxol or nocodazole (16 h). FLAG-tagged proteins were immunoprecipitated, then probed with anti-p-S377 antibody. (C) HEK293T cells transfected with FLAG-AMPKβ1-WT or FLAG-AMPKβ1-T19A and treated with taxol or nocodazole (16 h). FLAG-tagged proteins were immunoprecipitated, then probed with anti-p-T19 antibody. (D) HEK293T cells transfected with HA-AMPKα1-WT or HA-AMPKα1-2A (T382A/T490A) and treated with taxol or nocodazole (16 h). HA-tagged proteins were immunoprecipitated, then probed with anti-p-T490 antibody. (E) HEK293T cells transfected with HA-AMPKα1-WT or HA-AMPKα1-2A and treated with nocodazole (16 h) or nocodazole (16 h) with RO3306 and MG132 (1 h). HA-tagged proteins were immunoprecipitated, then probed with anti-p-T490 antibody. (F,G) HEK293T cells were transfected as indicated. At 48 h post-transfection, immunoprecipitated samples or total cell lysates were subjected to western blotting with antibodies against the indicated proteins. GFP-cyclin B1 is a constitutive active form of GFP-tagged cyclin B1 (R42A non-degradable mutant). (H) Co-immunoprecipitation of HA-tagged protein in HEK293T cells co-transfected with Myc-AMPKγ1, either HA-AMPKα1-WT or HA-AMPKα1-2A, and FLAG-AMPKβ1-WT or FLAG-AMPKβ1-T19A in HEK293T cells treated with nocodazole, then probed with antibodies against the indicated proteins. (I) Total lysates of HEK293T cells transfected with FLAG-AMPKα2-WT or FLAG-AMPKα2-K45R and treated with nocodazole, probed with anti-p-S377 antibody. (J) HeLa cells were synchronized by a double thymidine (DT) block-and-release method and collected at the indicated time points. AMPKα2 proteins were immunoprecipitated and subjected to western blotting with antibodies against the indicated proteins. Increased p-Aurora A levels mark cells in mitosis. (K) Immunofluorescence staining of p-S377 AMPKα2 in freely cycling HeLa cells stably expressing AMPKα2-WT or AMPKα2-2A (S377A/T485A). White arrows mark cells in metaphase or anaphase (condensed and aligned chromosomes). Orange arrows mark cells in interphase or cytokinesis.

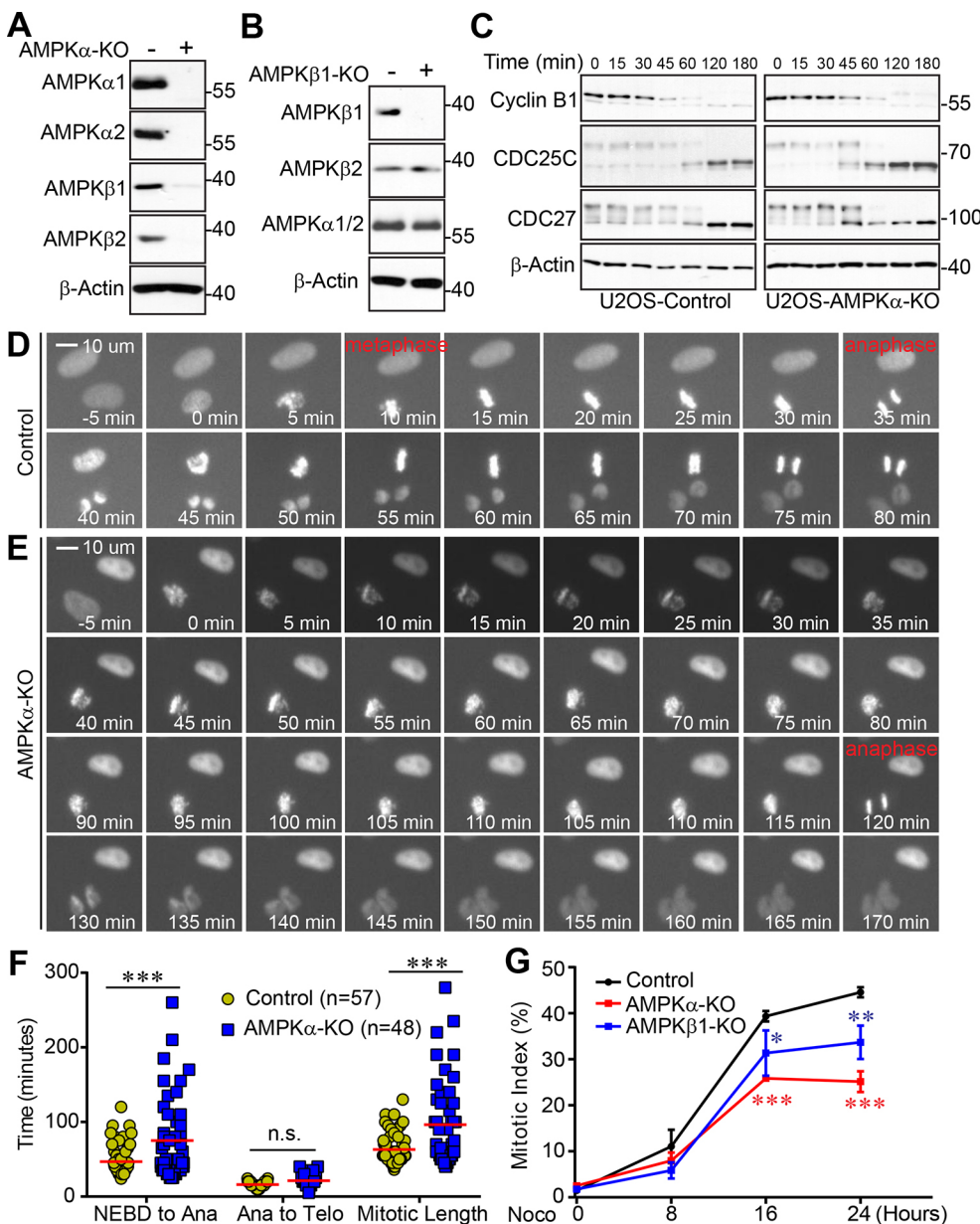


Fig. 4. AMPK is required for normal mitotic entry and progression.

(A,B) Western blots of U2OS, U2OS AMPK β 1-KO and U2OS AMPK α -KO (AMPK α 1/ α 2 double KO) cells probed for various AMPK subunits as indicated. (C) U2OS cells arrested in mitosis with nocodazole (16 h) which were subsequently washed and released into fresh medium for collection at the specified time points and then probed with antibodies against the indicated proteins. (D,E) Live-cell imaging of RFP-H2B-expressing U2OS or U2OS AMPK α -KO cells entering and exiting mitosis. (F) Quantification of mitotic phase timing from live-cell data. *** P <0.001 (two-way ANOVA); n.s., not significant. (G) Mitotic index time-course measurements of U2OS cells, U2OS AMPK β 1-KO cells and U2OS AMPK α -KO cells treated with nocodazole. Data were expressed as mean \pm s.e.m. from three independent experiments. * P <0.05, ** P <0.01, *** P <0.001 (two-tailed, unpaired Student's t -test). Scale bars: 10 μ m.

noticeable differences were seen in the rates of degradation of cyclin B1 or dephosphorylation of CDC25C and CDC27 between U2OS AMPK α -KO and control cells (Fig. 4C). Subsequently, by way of fluorescence live-cell imaging, we examined mitotic entry and progression of parental and AMPK α -KO U2OS cells stably expressing RFP-H2B. The parental U2OS cells quickly condensed their chromatin and aligned their chromosomes in a tightly packed metaphase plate within 15 min. Anaphase onset occurred 35 min after nuclear envelope break down (NEBD), with telophase, measured by chromatin decondensation, occurring at 50 min post-NEBD (Fig. 4D, upper). AMPK α -KO cells, in contrast, have a marked delay in aligning their chromosomes at metaphase, ~115 min after NEBD, and a postponement of anaphase onset to 120 min post-NEBD (Fig. 4E, lower). Quantitative analysis revealed that AMPK α -KO cells had 77% longer mitotic (NEBD to anaphase) duration than controls (Fig. 4F). Unsurprisingly, AMPK α -KO cells had a significantly longer mitotic duration, which concurs with a previous live-cell study using bright-field microscopy that specified a significantly increased mitotic duration for AMPK siRNA-treated

HeLa cells (Thaiparambil et al., 2012). Of note, similar anaphase-to-telophase timing in U2OS control and AMPK α -KO cells reinforces our earlier observation of unhindered mitotic exit in these cells (Fig. 4D–F). We noticed fewer rounded-up cells in the AMPK α -KO and AMPK β 1-KO cells when treated with taxol or nocodazole, so we performed cell cycle analysis using propidium iodide and found that there was no significant difference in the percentages of mitotically arrested cells between the knockouts and the controls (Fig. S1). Next, we stained U2OS control, AMPK α -KO and AMPK β 1-KO cells (treated with or without nocodazole for 0, 8, 16 or 24 h) with fluorescently labeled anti-phospho-histone H3 (S10) antibody to measure the mitotic index. Surprisingly, the number of mitotic cells in AMPK α -KO and AMPK β 1-KO U2OS, when treated for 16 or 24 h with nocodazole, was significantly lower than that of parental U2OS, indicating these cells may not be entering mitosis, but, having completed S-phase, have 4N DNA content (Fig. 4G).

Pharmacological abrogation of AMPK activity through use of small molecule inhibitors has been used widely for the study of AMPK function (Thaiparambil et al., 2012; Mao et al., 2013; Lee

et al., 2015; Wei et al., 2012). We utilized the Compound C and a newly identified AMPK-specific inhibitor SBI-0206965, which has been demonstrated to have an entirely different set of potential off-target kinases inhibited compared to Compound C (Dite et al., 2018). Abrupt inhibition of AMPK in RFP-H2B-expressing U2OS cells was accomplished with treatment with 5 μ M SBI-0206965 or 5 μ M Compound C, which were then immediately imaged for 24 h and the timing of each mitotic phase was analyzed. Similar to AMPK-KO cells, cells in which AMPK activity was inhibited displayed distinctly increased metaphase durations (Fig. 5A,B), demonstrating the importance of AMPK kinase activity for timely mitotic progression. From this, we wanted to further investigate why these cells were getting delayed at metaphase. Examination via confocal microscopy of U2OS cells with either genetic or pharmacological inhibition of AMPK kinase function revealed that a vast majority of AMPK-KOs or U2OS cells treated with Compound C fail to properly align their chromosomes during metaphase (Fig. 5C). Representative images are shown in Fig. 5D, displaying misaligned chromosomes frequently seen as far away from the metaphase plate as the centrosomes. The observed metaphase arrest in cells lacking functioning AMPK could be due to, in part, how chromosomes with kinetochores improperly attached to the mitotic spindle activate the spindle assembly checkpoint (SAC), which delays anaphase sister-chromatid separation until each chromosome is properly aligned and attached to the spindle (Lara-Gonzalez et al., 2012; Musacchio and Salmon, 2007).

AMPK phosphorylation is required for mitotic progression

The necessity of AMPK α expression for mitotic entry and proper prophase-to-anaphase progression prompted us to investigate the role of the two mitotic CDK1-mediated phosphorylation events of AMPK α , S377 and T490. For this, we generated stable cell lines expressing either AMPK α 1-WT or AMPK α 1-2A in the AMPK α -KO U2OS cells (Fig. 6A), with expression of AMPK α 1 WT or 2A near the levels found in parental U2OS cells rescuing the expression of both AMPK β subunits. Measurement of the mitotic index of U2OS AMPK α -KO cells treated with nocodazole, once again, revealed a concomitant drop in cells that lack AMPK expression arrested in mitosis. This could be fully rescued by the expression of AMPK α 1-WT, but only partially by the mitotic phosphorylation-null AMPK α 1-2A (Fig. 6B), indicating that AMPK α 1 could be the primary mitotic subunit in these cells and that mitotic phosphorylation by CDK1 may be important for proper progression into mitosis. We also created AMPK α 2-WT, AMPK α 1-K45R (kinase-dead) and AMPK α 1-T183A (phospho-activation-null) add-backs to the AMPK α -KO background (Fig. 6C). Expression of each form of AMPK α subunit were sufficient for recovering the expression of both AMPK β subunits (Fig. 6C). Analysis of the mitotic index of the AMPK α 1-K45R and AMPK α 1-T183A mutants showed the same significant decrease in mitotic cells as seen with AMPK α -KO (Fig. 6D), demonstrating that both AMPK kinase activity and activation at T183 are required for mitotic arrest. AMPK α 2-WT expression was only able to partially increase the suppressed phosphorylation of S10 on histone H3

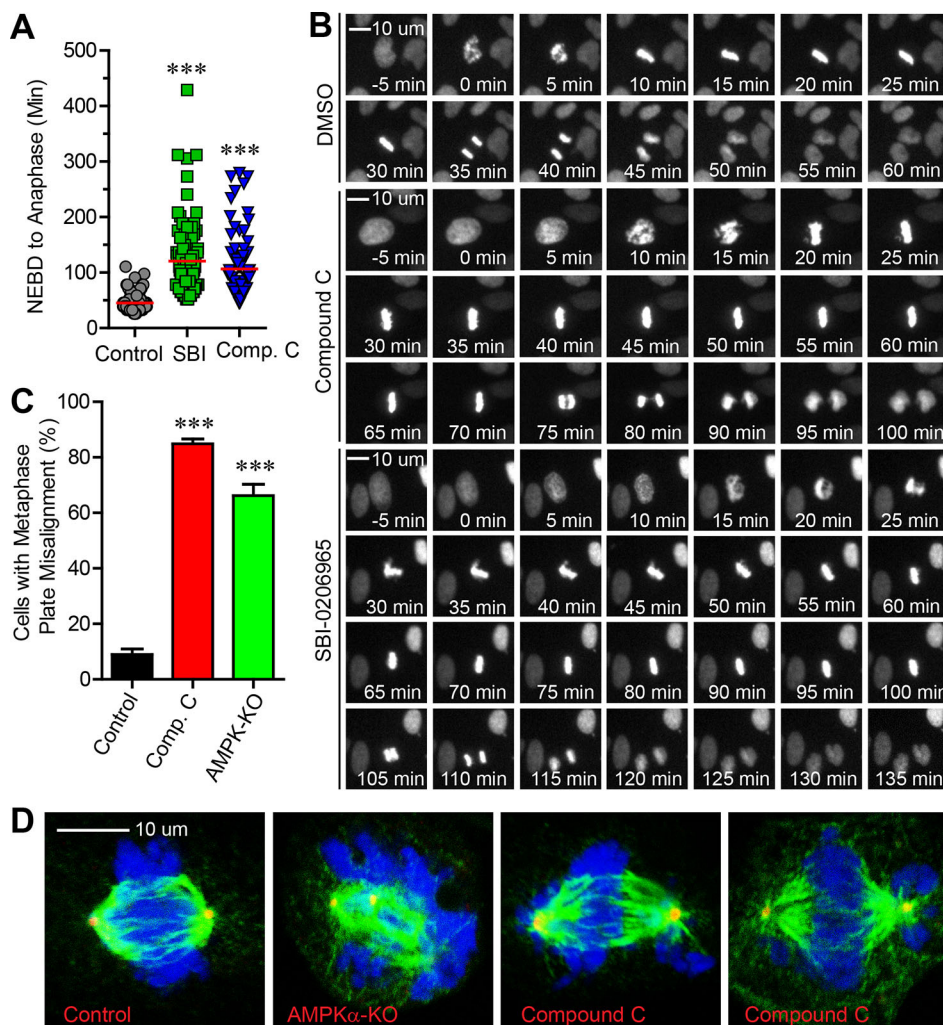


Fig. 5. Small-molecule inhibition of AMPK kinase activity phenocopies AMPK α -KO. (A) Live-cell image quantification of nuclear envelope breakdown (NEBD) to anaphase duration in RFP-H2B-expressing U2OS cells treated with 5 μ M SBI-0206965 (SBI) or 5 μ M Compound C (Comp. C) for 24 h. *** P <0.001 (two-tailed, unpaired Student's t -test). 100 cells were analyzed for each group in four separate experiments. (B) Representative live-cell images demonstrating duration of mitosis in cells quantified in A. (C) Quantification of abnormal metaphase plate alignment in confocal microscopy images (as shown in D) of fixed AMPK α -KO U2OS or U2OS cells treated with Comp. C. Data were expressed as mean \pm s.e.m. from four independent experiments. *** P <0.001 (two-tailed, unpaired Student's t -test). Total cells analyzed: control n =102, Comp. C n =103, AMPK α -KO n =122 in four separate experiments. (D) Representative confocal images of cells analyzed in C. DAPI is blue, α -tubulin is green and γ -tubulin is red. Scale bars: 10 μ m.

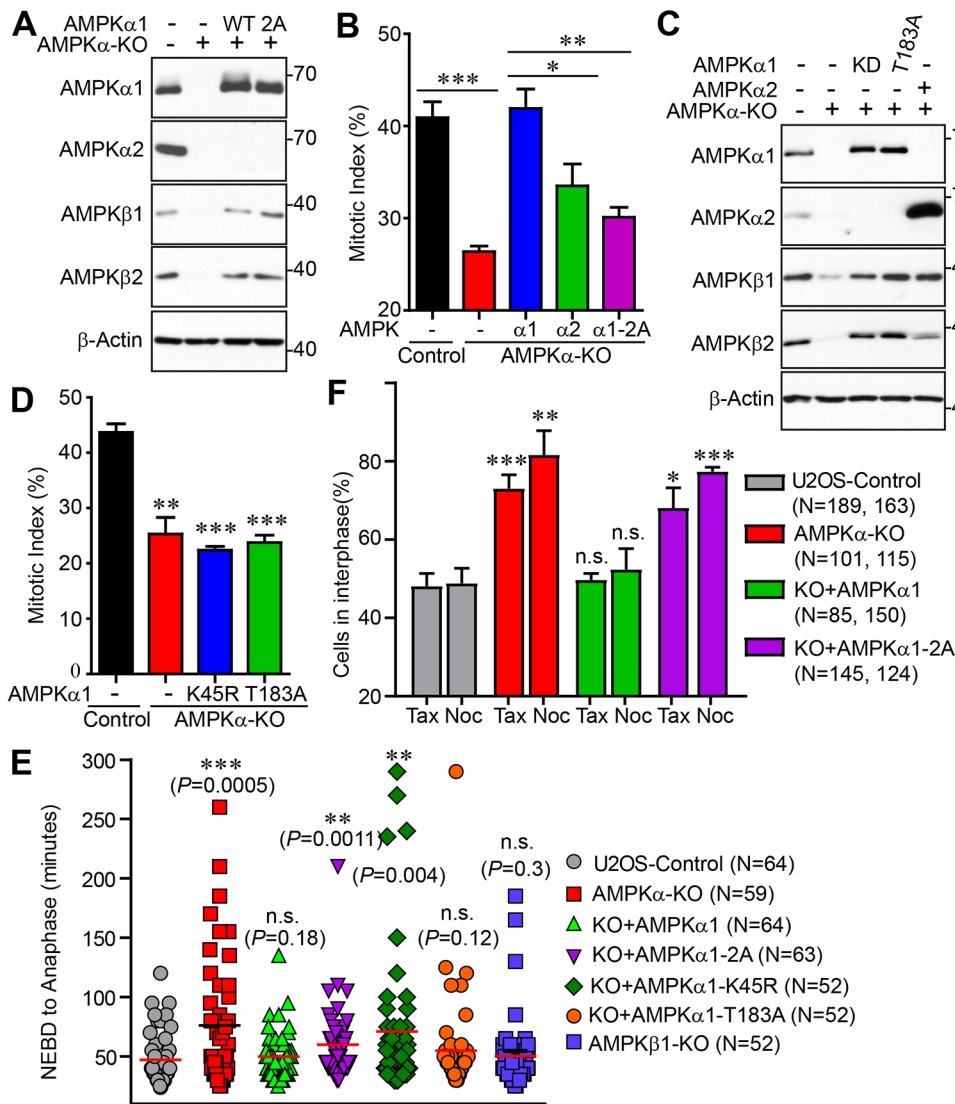


Fig. 6. AMPK α 1 re-expression can rescue AMPK α -KO mitotic phenotypes. (A) Western blots of U2OS AMPK α -KO cells stably expressing AMPK α 1-WT or AMPK α 1-2A, probed for various AMPK subunits as indicated. (B) Mitotic index of cells treated with nocodazole (16 h). Data were expressed as mean \pm s.e.m. from three independent experiments. * P <0.05, ** P <0.01, *** P <0.001 (two-tailed, unpaired Student's t -test). (C) Western blots of U2OS AMPK α -KO cells stably expressing AMPK α 1-K45R (KD), AMPK α 1-T183A or AMPK α 2-WT, probed for various AMPK subunits as indicated. (D) Mitotic index of cells treated with nocodazole (16 h). Data were expressed as mean \pm s.e.m. from three independent experiments. ** P <0.01, *** P <0.001 (two-tailed, unpaired Student's t -test). (E) Quantification of mitotic phase timing from live-cell imaging of RFP-H2B-expressing cells entering and exiting mitosis for 24 h. * P <0.01, *** P <0.001 (Mann-Whitney U -test). U2OS n =64, AMPK α -KO n =59, AMPK α 1-WT n =64, AMPK α 1-2A n =63, AMPK α 1-K45R n =52, AMPK α 1-T183A n =52, AMPK β 1-KO n =52. n.s., not significant. (F) Quantification of live-cell imaging of the percentage of cells (as indicated) remaining in interphase when treated with nocodazole for 24 h. Data were expressed as mean \pm s.e.m. from four independent experiments. * P <0.05, ** P <0.01, *** P <0.001 (two-tailed, unpaired Student's t -test). Total cells analyzed: U2OS taxol n =189, U2OS nocodazole n =163, AMPK α -KO taxol n =101, AMPK α -KO nocodazole n =115, α 1-WT taxol n =85, α 1-WT nocodazole n =150, α 1-2A taxol n =145 and α 1-2A nocodazole n =124 in four separate experiments. n.s., not significant.

(Fig. 6B). We next sought to elucidate the roles played by AMPK mitotic phosphorylation, kinase activity and phospho-activation in mitotic progression by stably expressing RFP-H2B in each AMPK α 1 mutant and the AMPK β 1-KO cell lines, following unperturbed mitoses, and determining the timing of mitotic entry to anaphase onset. Interestingly, AMPK α 1-WT and AMPK α 1-T183A could fully rescue the prometaphase delay seen in AMPK α -KO cells (Fig. 6E). In addition, knocking out AMPK β 1 had no effect on metaphase alignment or the interval from NEBD to anaphase. By contrast, AMPK α 1-K45R could not rescue and AMPK α 1-2A could only partially rescue the prolonged arrest during prometaphase/metaphase (Fig. 6E), indicating that AMPK kinase activity is required, and CDK1 mitotic phosphorylation is, at least in part, essential for proper early mitotic progression. Since we saw that the AMPK α -KOs, when treated for 16 h with nocodazole, were indeed accumulating with 4N DNA content and were pH3 (S10)-negative, we then wanted to confirm whether these cells were endoreduplicating or simply never entering mitosis. To do this, we used fluorescence live-cell microscopy to follow individual cells under the treatment of taxol or nocodazole for 48 h. Remarkably, 73–81% of AMPK α -KO cells persisted in interphase and never arrested in mitosis, which was significantly higher than parental U2OS cells in which only 48–49% remained in interphase (Fig. 6F). In contrast, AMPK α 1-WT

expression partially rescued and cleared more cells to progress into mitosis, so only 49–52% remained unarrested, whereas AMPK α 1-2A was more like AMPK α -KO with 68–77% lingering in interphase (Fig. 6F). These data confirmed that CDK1-mediated phosphorylation of, and the kinase activity by, AMPK is not only important for faithful mitotic entry, but also for proper progression to DNA segregation at anaphase.

AMPK phosphorylation regulates transcription of genes involved in mitosis

To get insight into the downstream signaling of AMPK, we next investigated the transcriptome of U2OS cells by next-generation RNA sequencing (RNA-seq). Comparative analysis of parental U2OS (control) versus AMPK α -KO and control versus AMPK α 1-2A cells was performed using ingenuity pathway analysis (IPA) to examine canonical pathways similarly altered in each to designate effects due to dysregulation of CDK1 phosphosites. Intriguingly, canonical pathways influencing actin dynamics such as actin cytoskeleton signaling, ILK signaling and regulation of actin-based motility by Rho were predicted to be significantly activated (Fig. 7A). Unsurprisingly, the expression of a multitude of genes involved in promoting cellular movement and migration were increased and several inhibitors of cell movement were diminished in AMPK α -KO and AMPK α 1-2A

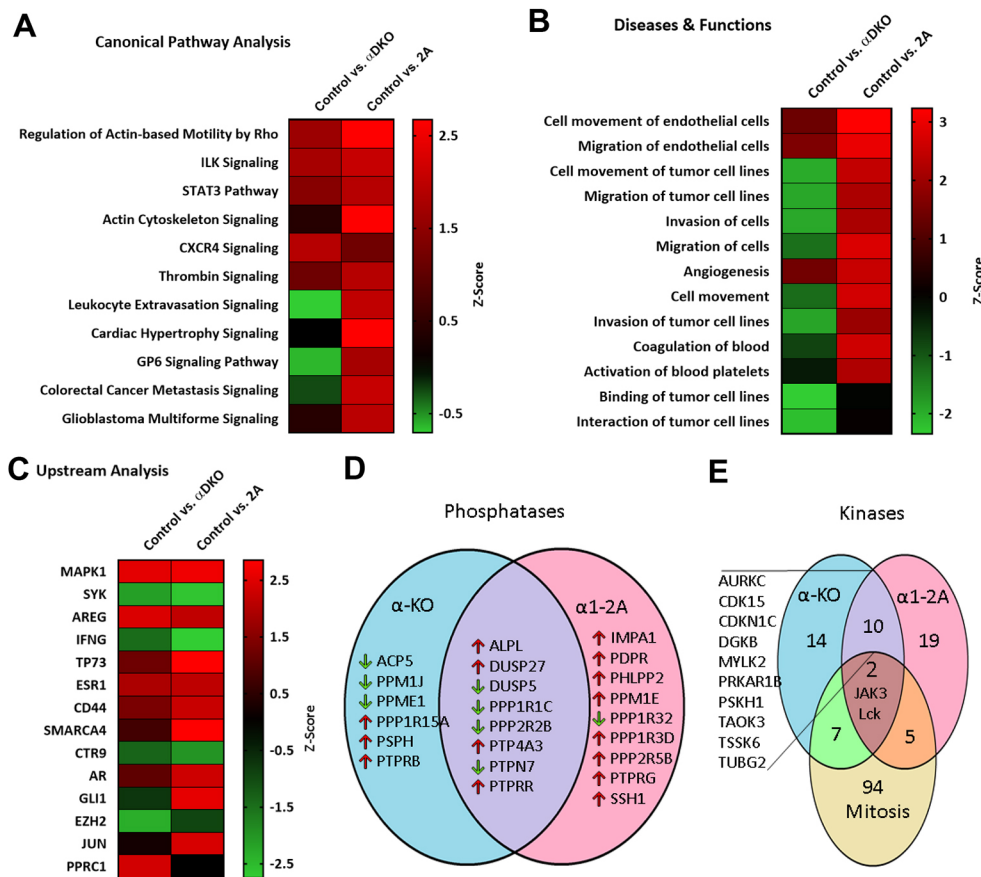


Fig. 7. RNA-seq analysis of AMPK α -KO and AMPK α 1-2A U2OS cells. (A) Top canonical pathways altered in AMPK α -KO and AMPK α -KO reconstituted with AMPK α 1-2A U2OS cells derived from ingenuity pathway analysis (IPA) gene ontology algorithms. (B) Top diseases and biological functions found enriched in AMPK α -KO and AMPK α 1-2A reconstituted U2OS cells. (C) Upstream regulators predicted to be activated or inhibited based on genes that were significantly different for parental U2OS and AMPK α -KO or AMPK α 1-2A reconstituted U2OS cells. (D) Comparison of phosphatases altered more than twofold in AMPK α -KO and AMPK α 1-2A reconstituted U2OS cells. (E) Kinases identified by IPA gene ontology algorithms as mitotic kinases compared with kinases altered more than twofold in AMPK α -KO and AMPK α 1-2A reconstituted U2OS cells.

cells compared to controls (Fig. 7B). By examining alterations of downstream gene expression, upstream analysis pinpointed numerous possible upstream regulators. Most of the highest-scoring upstream effectors were analogously modulated between AMPK α -KO and AMPK α 1-2A compared to controls (Fig. 7C), indicating that loss of phosphorylation of AMPK by CDK1 is comparable to AMPK knockout for alterations seen in these particular pathways. We previously detected stark reduction of p-histone H3 (S10) in both the AMPK α -KO and AMPK α 1-2A cells, which led us to speculate that this was possibly due to either phosphatase dysregulation leading to hyper-dephosphorylation or perturbation of kinase signaling leading to inadequate phosphorylation of histone H3. Interestingly, there were eight significantly up- or downregulated phosphatases found to be changed mutually between the AMPK α -KO and AMPK α 1-2A cells compared to controls (Fig. 7D). Furthermore, between the two treatments, the expression levels of ten kinases and two mitosis-associated kinases significantly changed compared to controls (Fig. 7E).

AMPK phosphorylation potentiates taxol cytotoxicity

Taxanes and similar compounds rely on the disruption of microtubule dynamics in order to arrest cells in mitosis through activation of the SAC, with the prolonged arrest triggering cell death through a unique anti-proliferative process called mitotic cell death (Vitale et al., 2011) or through aberrant mitosis and eventual death in G₁ (Abal et al., 2003). Because of this method of action, cancer cells must enter mitosis in order to suffer the effects of taxol and eventually succumb to cell death mechanisms. With this in mind, we next had to ascertain whether loss of AMPK activity could indeed provide cancer cells with a means to resist cell death by taxol treatment. AMPK α -KO cells, compared to parental U2OS cells, had distinctly reduced levels

of apoptosis, as revealed by cleaved PARP. Addition of AMPK α 1-WT amply rescued and resensitized the cells, whereas AMPK α 1-2A had muted levels of cleaved PARP similar to AMPK α -KO (Fig. 8A), suggesting that cells lacking AMPK α expression have a proclivity to resist taxol-mediated mitotic cell death. Similar resistance was seen in MCF7 and SKBR3 breast adenocarcinoma cells when treated concomitantly with taxol or vinblastine (a microtubule destabilizing agent) and SBI-0206965. Both cell types displayed high cleaved PARP protein levels under taxol or vinblastine treatment alone. Yet, when AMPK was inhibited in MCF7 and SKBR3 cells exposed to these drugs for 24 h, substantial reductions in cleaved PARP were seen (Fig. 8B), evidencing that AMPK activity is necessary for significant levels of apoptosis elicited by anti-tubulin mitotic arrest. Both SBI-0206965 and Compound C could significantly reduce the mitotic index of HeLa cells that were treated with taxol compared to taxol treatment alone (Fig. 8C,D), signifying that the lack of apoptosis in these cells is possibly due to AMPK inhibition blocking mitotic entry and thus protecting cancer cells from mitotic cell death and apoptosis triggered by paclitaxel. Survival curves for breast cancer patients who received systemic treatments and who had high AMPK α 1 expression displayed significantly higher relapse-free survival (RFS) rates than survival curves for patients who had low AMPK α 1 expression (Györfy et al., 2010) (Fig. 8E). Interestingly, there is no difference in RFS for patients with high or low AMPK α 2 or AMPK β 2 expression, but a moderately higher RFS rate in patients expressing high levels of AMPK β 1 (Fig. 8F–H).

DISCUSSION

AMPK has previously been reported to have increased phosphorylation levels at the T172 activation site during mitosis (Vazquez-Martin et al., 2009; Thaiparambil et al., 2012; Mao et al.,

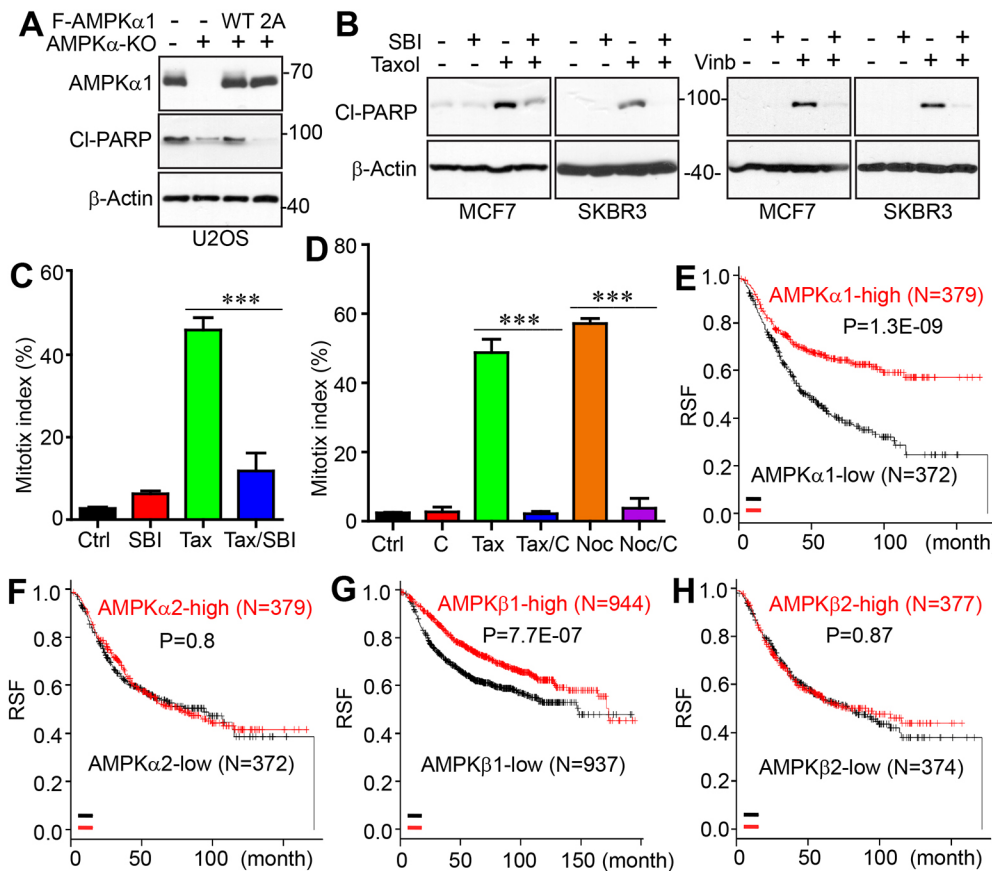


Fig. 8. AMPK expression and kinase activity are crucial for paclitaxel drug sensitivity and breast cancer patient relapse-free survival. (A) Western blot of U2OS, AMPK α -KO, AMPK α 1-WT and AMPK α 1-2A cells treated with taxol (100 nM) for 24 h and probed for cleaved PARP. (B) Western blot of MCF7 and SKBR3 cells treated with SBI-0206965 (SBI, 1 μ M), and taxol (500 nM and 100 nM, respectively) or vinblastine (Vinb, 5 ng/ml) for 24 h and probed for cleaved PARP. (C) Mitotic indexes of HeLa cells treated with taxol alone, SBI alone or taxol with SBI. (D) Mitotic indexes of HeLa cells treated with taxol alone, nocodazole alone, Compound C (C) alone, taxol with Compound C or nocodazole with Compound C. Data in C,D are expressed as mean \pm s.e.m. from three independent experiments. *** P <0.001 (two-tailed, unpaired Student's t -test). (E–H) Kaplan–Meier curves of relapse-free survival versus *PRKAA1* (AMPK α 1) (E), *PRKAA2* (AMPK α 2) (F), *PRKAB1* (AMPK β 1) (G) and *PRKAB2* (AMPK β 2) (H) expression in breast cancer patients treated systemically. Data were generated using an online survival analysis tool, KM Plotter (<https://kmplot.com/analysis/>), using microarray data from 1809 patients (Györfy et al., 2010).

2013; Banko et al., 2011; Pinter et al., 2012). The current study is the first to identify direct phosphorylation sites outside of T172 on the AMPK complex, targeted by a bona fide mitotic kinase. These phosphorylations by CDK1 on the AMPK α 1, α 2 and β 1 subunits, seen *in vitro* and in cells, adds a novel upstream kinase to the group of known AMPK phospho-regulators. CDK1 phosphorylation of AMPK α 2 at S377/T485 and AMPK α 1 at T490, as well as of AMPK β 1 at T19, was seen to be highly enriched in cells arrested in mitosis by anti-mitotic drugs, which could be abolished by addition of CDK1-specific inhibitors. The reduced mitotic index in AMPK α -KO cells when treated with taxol or nocodazole was, interestingly, due to their lack of mitotic entry when individual cells were monitored using live-cell imaging. This could be rescued by reconstitution of AMPK α 1-WT, but not AMPK α 1-2A, providing evidence that AMPK activity and CDK1 phosphorylation is important for cellular entry into mitosis. It has been reported that AMPK phosphorylation of GBF1 is required for mitotic entry through regulation of mitotic Golgi fragmentation (Mao et al., 2013; Lee et al., 2015), so it may be through this process or through other, as-yet-undiscovered, means by which AMPK phosphorylation by CDK1 promotes mitotic entry.

The IPA analysis of RNA-seq data of AMPK α -KO and AMPK α 1-2A cells compared to controls revealed multiple pathways, functions and upstream effectors that are modified by loss of CDK1 phospho-regulation. From this, the predicted activation of mitogen-activated protein kinase 1 (MAPK1) could conceivably be driven through stimulation of actin cytoskeleton signaling (Hoffman et al., 2017). Furthermore, the spleen tyrosine kinase (SYK) and interferon gamma (IFNG) downregulation similarly seen in both knockout and CDK1 phosphorylation-null AMPK cells is of importance due to each gene's role in suppression

of tumorigenesis in breast carcinoma (Coopman et al., 2000) and promotion of apoptosis (Ruiz-Ruiz et al., 2000), respectively. Stimulation of amphiregulin (AREG) signaling is of note because it promotes cancer growth through interactions with EGF and/or TGF α receptors (Salomon et al., 1995). Likewise, high SWI/SNF-related matrix-associated actin-dependent regulator of chromatin 4 (SMARCA4) activity has been seen to promote tumor cell proliferation and is associated with poor prognosis in multiple cancers (Chen et al., 2018; Guerrero-Martínez and Reyes, 2018) and has been reported to increase expression of CD44 (Banine et al., 2005), itself a promoter of resistance to apoptosis and important in breast cancer cell migration (Lakshman et al., 2004; Nam et al., 2015). Additionally, overactive tumor protein 73 (TP73) has also been implicated in poor clinical behavior and in promotion of tumorigenesis of breast carcinomas (Domínguez et al., 2001). Interestingly, estrogen receptor 1 (ESR1) upregulation has been associated with EZH2 downregulation (Reijm et al., 2011), both of which are seen to occur in AMPK α knockout and mitotic phosphorylation-null AMPK α 1-2A cells. High estrogen receptor (ER) expression has been associated with increased proliferation and higher grade breast cancer (Moelans et al., 2011). Androgen receptor (AR) overexpression in triple-negative breast cancers can allow a switch from ER-dependence to AR-dependence, which results in resistance to aromatase inhibitor treatments (Fujii et al., 2014). Further, phosphatases such as ALPL and PTP4A3, which are increased in late-stage and aggressive triple-negative breast cancers, have been found to be indicative of poor patient survival and have been discovered to be promoters of cancer cell proliferation (Singh et al., 2013; den Hollander et al., 2016). Importantly, suppression of DUSP5 expression is correlated with paclitaxel resistance and poor prognosis in basal-like breast cancer (Liu et al., 2018).

Other studies have shed some light on AMPK's role in mitosis through chemically inhibiting AMPK kinase activity. Compound C, a widely used AMPK inhibitor, has been shown to delay mitotic entry (Mao et al., 2013; Lee et al., 2015), cause spindle misorientation and misattachment of chromosomes through actin bundling, and to increase mitotic duration as measured from mitotic rounding to cytokinesis via bright-field microscopy (Thaiparambil et al., 2012; Wei et al., 2012). Correspondingly, we found that inhibition of AMPK kinase activity using Compound C or a newly described AMPK-specific inhibitor, SBI-0206965 (Dite et al., 2018), results in significantly delayed progression through mitosis from NEBD to anaphase and is marked by a profound degree of chromosomal misalignment. Our results have also shown that AMPK inhibitors can constrain the killing ability of anti-tubulin drugs in breast cancer cells through blocking mitotic entry. This is significant because cells must proceed into mitosis in order for the mechanism of taxol microtubule stabilization to lead to mitotic arrest and eventual cell death, indicating that in breast cancer patients, use of AMPK inhibitors is contraindicated.

Metformin, the common anti-diabetic drug for treating type 2 diabetes and activator of AMPK, has been shown to cause cell cycle arrest, suppress anchorage-dependent growth and inhibit cell proliferation in breast cancer cell lines (Zakikhani et al., 2006; Alimova et al., 2009; Liu et al., 2009). Additional studies suggest that metformin may improve the efficacy of breast cancer treatments and regimens, as well as selectively target and kill cancer stem cells (Vazquez-Martin et al., 2009; Hirsch et al., 2009; Oliveras-Ferraro et al., 2009). Metformin has also been shown to constrain mammary tumor expansion in mice (Anisimov et al., 2005). This fact has led to the dozens of clinical trials exploring the use of metformin as a neoadjuvant, in combinatorial chemotherapies or as a chemoprevention agent (Kasznicki et al., 2014). Indeed, several clinical phase II and phase III trials have recently been initiated to examine the synergistic effects of treatment with metformin and other drugs used in cytotoxic chemotherapy, such as docetaxel or paclitaxel. These were initiated after meta-analysis of retrospective studies identified the use of metformin with a significant reduction in cancer-related mortality for patients (Chae et al., 2016; Marrone et al., 2018). Our analysis of patient data revealed that breast cancer patients who had high AMPK α 1 or AMPK β 1 expression and received systemic treatments displayed significantly higher RFS rates than patients who had low AMPK α 1 or AMPK β 1 expression (Györfy et al., 2010). This strongly indicates the use of metformin in breast cancer treatment regimens, especially in patients with tumors expressing low levels of the mitotically phosphorylated AMPK subunits, AMPK α 1 and AMPK β 1, in order to improve their survival.

In conclusion, we propose that CDK1 regulates AMPK control of mitotic entry and progression. It remains to be determined which signaling networks or processes CDK1-phosphorylated AMPK utilizes to drive these events. Thus, future studies will need to examine whether this newly identified CDK1-AMPK axis is involved in Golgi fragmentation, mitotic spindle orientation or some other currently unassociated mitotic process.

MATERIALS AND METHODS

Cell culture and transfection

HEK293T, HeLa, U2OS, MCF7 and SKBR3 cell lines were purchased from American Type Culture Collection (ATCC) and cultured as ATCC instructed. The cell lines were authenticated at ATCC and were used at low (<25) passages. Attractene (Qiagen) was used for transient overexpression of proteins in HEK293T cells following the manufacturer's instructions. Lentivirus packaging, infection and subsequent selection were done as we

have described previously (Stauffer et al., 2016). Nocodazole (100 ng/ml for 16 h) and taxol (100 nM for 16 h) (Selleck Chemicals) were used to arrest cells in mitosis unless otherwise indicated. Kinase inhibitors were purchased from Selleck Chemicals (VX680, BI2536, purvalanol A, SP600125, SB216736, SBI-0206965 and MK-2206), ENZO life Sciences (RO3306) or LC Laboratory (U0126 and SB203580). All other chemicals were from either from Sigma-Aldrich or Thermo Fisher.

Expression constructs

Human pcDNA3-HA-AMPK α 1-WT and Myc-AMPK γ 1-WT constructs were a gift from Dr Ken Inoki, University of Michigan, Ann Arbor, MI, USA (Inoki et al., 2003). Human pECE-HA-AMPK β 1-WT and pECE-HA-AMPK α 2-WT were deposited by Anne Brunet (Addgene plasmids #31666 and #31654) (Banko et al., 2011). pLKO.1-H2B-RFP was deposited by Elaine Fuchs (Addgene plasmid #26001) (Beronja et al., 2010). Point mutations were generated by the QuikChange Site-directed PCR mutagenesis kit (Stratagene) and verified by Sanger sequencing. Retroviral expression constructs were made by cloning full-length AMPK β 1 or AMPK α 2 cDNA into MaRXTMIV (Xiao et al., 2011). Lentiviral expression constructs were generated by cloning full length AMPK α 2 cDNA into pSIN4-FLAG-IRES-Puro or AMPK α 1 into pSIN4-FLAG-IRES-Neo (Stauffer et al., 2017).

EGFP-expressing all-in-one CRISPR construct

To construct the all-in-one CRISPR/Cas9n plasmid targeting AMPK β 1, the sense and anti-sense oligonucleotides from Table S1 were synthesized, annealed and Golden Gate-assembled into the pX330A_D10A-1 \times 2-EGFP and pX330S-2 vectors as described previously (Stauffer et al., 2017). After the two vectors were generated, a final Golden Gate assembly was performed to generate the all-in-one vector as described previously (Sakuma et al., 2014). The resulting pX330A_D10A-1 \times 2-EGFP-PRKAB1-AB construct was transfected into cells and GFP-positive clones were selected by flow cytometry-based cell sorting.

To construct the all-in-one CRISPR/Cas9n plasmid targeting both AMPK α 1 and AMPK α 2, the sense and anti-sense oligonucleotides from Table S1 were synthesized, annealed and Golden Gate-assembled into the pX330A_D10A-1 \times 2-EGFP, pX330S-2, pX330S-3 and pX330S-4 (Stauffer et al., 2017). After the four vectors were generated, a final Golden Gate assembly was performed to generate the all-in-one vector. The resulting pX330A_D10A-1 \times 2-EGFP-PRKAA1/2-ABCD construct was transfected into U2OS cells and GFP-positive clones were selected by flow cytometry-based cell sorting.

Recombinant protein purification and *in vitro* kinase assay

GST-tagged AMPK α 2-WT and AMPK α 2-2A, as well as GST-tagged AMPK β 1-WT, T19A, S40A and 2A were cloned into pGEX-5X-1. Proteins were bacterially expressed and purified on GSTrap FF affinity columns (GE Healthcare) following the manufacturer's instructions. GST-AMPK α 2 or GST-AMPK β 1 (0.5–1 μ g) was incubated with 10 U recombinant CDK1-cyclin B complex (New England Biolabs) or 100 ng CDK1/cyclin B (SignalChem) in kinase buffer (New England Biolabs) in the presence of 5 μ Ci γ -³²P-ATP (3000 Ci/mmol, PerkinElmer). PLK1 kinase was also obtained from SignalChem. Phosphorylation was visualized by autoradiography (³²P incorporation) followed by western blotting or detected by phospho-specific antibodies.

Antibodies

Rabbit polyclonal antibody against p-T485/T490 AMPK α 1/2 (1:1000) was a gift from Dr Ken Inoki (Suzuki et al., 2013). Antibodies against AMPK α 1 (1:2000, 2795), AMPK α 2 (1:2000, 2757), AMPK β 1 (1:2000, 4178), AMPK β 2 (1:2000, 4148), AMPK γ 1 (1:2000, 4187), AMPK γ 2 (1:2000, 2536), AMPK γ 3 (1:2000, 2550), AMPK α 1/ α 2 (1:2000, 2532), p-AMPK α (T172) (1:1000, 2535), p-AMPK β 1 (S182) (1:1000, 4186), p-AMPK β 1 (S108) (1:2000, 4181), p-Aurora A/B/C (T288/T232/T198) (1:2000, 2914), CDC25C (1:2000, 4688), p-Histone H3 (S10) Alexa Fluor 488 (1:100, 3465) and cleaved PARP antibodies (1:2000, 5625) were from Cell Signaling Technology. Anti- β -actin (1:4000, sc-47778), anti-cyclin B1 (1:2000, sc-245) and anti-CDC27 (1:1000, sc-9972) antibodies were from Santa Cruz Biotechnology. Anti-FLAG (1:4000, F1804), anti-HA (1:2000,

H9658) and anti-Myc (1:1000, 05-419) antibodies were from Sigma-Aldrich. Anti- α -tubulin (1:300, ab15246) antibody was from Abcam. Anti- γ -tubulin (1:200, 629201) antibody was from Biolegend. Anti-p-AMPK α 2 (S377) (1:500) and anti-p-AMPK β 1 (T19) (1:1000) phospho-antibodies were generated and purified by AbMart. The phospho-peptides used for immunizing rabbits were PLIAD-pS-PKARC (p-AMPK α 2 S377) and HGGHK-pT-PRRDS (p-AMPK β 1 T19). Matching non-phosphorylated peptides were also synthesized and used for antibody purification and blocking assays.

Immunoprecipitation, Phos-tag and western blot analysis

Phos-tag was obtained from Wako Pure Chemical Industries (304-93521). Phos-tag gels were made using 10 μ M Phos-tag (with 100 μ M MnCl₂) in 8% SDS-acrylamide gels as described (Zhou et al., 2018). Immunoprecipitation, western blotting and lambda phosphatase treatment assays were done as previously described (Zeng et al., 2017).

Immunofluorescence staining and confocal microscopy

HeLa cells stably expressing AMPK α 2-WT or AMPK α 2-2A were used for immunofluorescence staining with the p-AMPK α 2 S377 antibody. Cell fixation, permeabilization, immunofluorescence staining and confocal microscopy were performed as previously described (Chen et al., 2016).

RNA extraction, construction of RNA libraries and RNA-Seq

We extracted RNA from AMPK α -KO and AMPK α -KO reconstituted with AMPK α 1-2A U2OS cells using the Direct-zol RNA Miniprep Plus Kit (Zymo Research) and evaluated the purity and concentration of the RNA by ultraviolet spectroscopy (NanoDrop). RNA integrity numbers (RIN) were evaluated using the Agilent 2100 Bioanalyzer. RNA sequencing libraries were constructed using 1000 ng of total RNA from each sample and the TruSeqV2 kit from Illumina following manufacturer's protocol. Illumina NextSeq sequencing and next-generation sequencing data acquisition were conducted at the UNMC Genomics Core Facility. The libraries were subjected to 75 bp paired-end high-output sequencing using a NextSeq500 sequencer to generate approximately 33.3 to 41.6 million reads per sample. Fastq files were generated using the bc12fastq software, version 1.8.4 and provided to the UNMC Bioinformatics Core facility for further analysis. The original fastq format reads were trimmed and filtered using the fqtrim tool (<https://ccb.jhu.edu/software/fqtrim>) to remove adapters, terminal unknown bases (Ns) and low quality 3' regions (Phred score < 30). The trimmed fastq files were processed by our facility's newly developed standard pipeline utilizing STAR (Dobin et al., 2013) as the aligner and RSEM (Li and Dewey, 2011) as the tool for annotation and quantification at both gene and isoform levels. TPM values were used for comparison results (Student's *t*-test) for all the available genes. The Benjamini-Hochberg (BH) adjusted *P*-values (Benjamini and Hochberg, 1995) were also provided to adjust for multiple testing-caused false discovery rate (FDR) with significant level of adjusted *P*-value of ≤ 0.05 .

Live-cell imaging

U2OS and lentiviral-transduced U2OS cells were plated on black 96-well optical bottom plates (Thermo Fisher). Live-cell imaging was performed in a Cellomics Arrayscan VTI HCS Reader with 37°C, 5% CO₂ incubation using FluroBrite DMEM (Thermo Fisher) supplemented with 4 mM L-glutamine, 10% FBS, 1% pen/strep. Cells were monitored for 24 h and pictures were taken every 5 min using an RFP filter. Measurements of cell cycle durations were done using the time-lapse sequences.

Statistical analysis

Statistical significance was analyzed using a two-tailed, unpaired Student's *t*-test or using a two-way ANOVA with the Šidák correction for multiple comparisons. A *P*-value of <0.05 was considered to indicate statistical significance.

Acknowledgements

We are very grateful to Dr Ken Inoki (University of Michigan, USA) for the anti-p-AMPK α 1/2 T490/T485 antibody and AMPK constructs. Dr Shuping Yang (Shandong University, China) helped generate the AMPK α 1-2A mutant. All

fluorescence images were acquired using Zeiss LSM 710 or LSM 800 confocal microscopes at the Advanced Microscopy Core at the University of Nebraska Medical Center. The core is supported in part by grant P30 GM106397 from the National Institutes of Health (NIH). RNA sequencing was performed at University of Nebraska DNA Sequencing Core. The core receives partial support from the National Institute for General Medical Science (NIGMS) INBRE - P20 GM103427-14 and COBRE - 1P30 GM110768-01 grants as well as The Fred & Pamela Buffett Cancer Center Support Grant - P30 CA036727. We also thank Dr Joyce Solheim for critical reading and comments on the manuscript.

Competing interests

The authors declare no competing or financial interests.

Author contributions

Conceptualization: J.D.; Methodology: S.S.; Formal analysis: S.S.; Investigation: S.S., Y.Z., M.S., J.Z., Y.C.; Data curation: S.S., Y.Z., M.S., J.Z., Y.C.; Writing - original draft: S.S.; Writing - review & editing: S.S., J.D.; Supervision: J.D.; Project administration: Y.C., J.D.; Funding acquisition: J.D.

Funding

Research in the Dong laboratory is supported by Fred & Pamela Buffett Cancer Center Support Grant (P30 CA036727), and National Institutes of Health grants P30 GM106397 and R01 GM109066. Deposited in PMC for release after 12 months.

Data availability

RNA-seq data has been deposited in the Gene Expression Omnibus under accession number GSE139293.

Supplementary information

Supplementary information available online at <http://jcs.biologists.org/lookup/doi/10.1242/jcs.236000.supplemental>

References

- Abal, M., Andreu, J. M. and Barasoain, I. (2003). Taxanes: microtubule and centrosome targets, and cell cycle dependent mechanisms of action. *Curr. Cancer Drug Targets* **3**, 193-203. doi:10.2174/1568009033481967
- Alimova, I. N., Liu, B., Fan, Z., Edgerton, S. M., Dillon, T., Lind, S. E. and Thor, A. D. (2009). Metformin inhibits breast cancer cell growth, colony formation and induces cell cycle arrest in vitro. *Cell Cycle* **8**, 909-915. doi:10.4161/cc.8.6.7933
- Anisimov, V. N., Egormin, P. A., Bershtein, L. M., Zabezhinskii, M. A., Piskunova, T. S., Popovich, I. G. and Semchenko, A. V. (2005). Metformin decelerates aging and development of mammary tumors in HER-2/neu transgenic mice. *Bull. Exp. Biol. Med.* **139**, 721-723. doi:10.1007/s10517-005-0389-9
- Bakhom, S. F. and Swanton, C. (2014). Chromosomal instability, aneuploidy, and cancer. *Front. Oncol.* **4**, 161. doi:10.3389/fonc.2014.00161
- Banine, F., Bartlett, C., Gunawardena, R., Muchardt, C., Yaniv, M., Knudsen, E. S., Weissman, B. E. and Sherman, L. S. (2005). SWI/SNF chromatin-remodeling factors induce changes in DNA methylation to promote transcriptional activation. *Cancer Res.* **65**, 3542-3547. doi:10.1158/0008-5472.CAN-04-3554
- Banko, M. R., Allen, J. J., Schaffer, B. E., Wilker, E. W., Tsou, P., White, J. L., Villén, J., Wang, B., Kim, S. R., Sakamoto, K. et al. (2011). Chemical genetic screen for AMPK α 2 substrates uncovers a network of proteins involved in mitosis. *Mol. Cell* **44**, 878-892. doi:10.1016/j.molcel.2011.11.005
- Benjamini, Y. and Hochberg, Y. (1995). Controlling the false discovery rate: a practical and powerful approach to multiple testing. *J. R. Stat. Soc. Ser. B* **57**, 289-300. doi:10.1111/j.2517-6161.1995.tb02031.x
- Beronja, S., Livshits, G., Williams, S. and Fuchs, E. (2010). Rapid functional dissection of genetic networks via tissue-specific transduction and RNAi in mouse embryos. *Nat. Med.* **16**, 821-827. doi:10.1038/nm.2167
- Chae, Y. K., Arya, A., Malecek, M. K., Shin, D. S., Carneiro, B., Chandra, S., Kaplan, J., Kalyan, A., Altman, J. K., Platanias, L. et al. (2016). Repurposing metformin for cancer treatment: current clinical studies. *Oncotarget* **7**, 40767-40780. doi:10.18632/oncotarget.8194
- Chen, X., Stauffer, S., Chen, Y. and Dong, J. (2016). Ajuba phosphorylation by CDK1 promotes cell proliferation and tumorigenesis. *J. Biol. Chem.* **291**, 14761-14772. doi:10.1074/jbc.M116.722751
- Chen, Z., Lu, X., Jia, D., Jing, Y., Chen, D., Wang, Q., Zhao, F., Li, J., Yao, M., Cong, W. et al. (2018). Hepatic SMARCA4 predicts HCC recurrence and promotes tumour cell proliferation by regulating SMAD6 expression. *Cell Death Dis.* **9**, 59. doi:10.1038/s41419-017-0090-8
- Coopman, P. J. P., do, M. T. H., Barth, M., Bowden, E. T., Hayes, A. J., Basyuk, E., Blancato, J. K., Vezza, P. R., Mcleskey, S. W., Mangeat, P. H. et al. (2000). The Syk tyrosine kinase suppresses malignant growth of human breast cancer cells. *Nature* **406**, 742-747. doi:10.1038/35021086
- Dasgupta, B. and Milbrandt, J. (2009). AMP-activated protein kinase phosphorylates retinoblastoma protein to control mammalian brain development. *Dev. Cell* **16**, 256-270. doi:10.1016/j.devcel.2009.01.005

- Daub, H., Olsen, J. V., Bairlein, M., Gnad, F., Oppermann, F. S., Körner, R., Greff, Z., Kéri, G., Stemmann, O. and Mann, M. (2008). Kinase-selective enrichment enables quantitative phosphoproteomics of the kinome across the cell cycle. *Mol. Cell* **31**, 438–448. doi:10.1016/j.molcel.2008.07.007
- Den Hollander, P., Rawls, K., Tsimelzon, A., Shepherd, J., Mazumdar, A., Hill, J., Fuqua, S. A. W., Chang, J. C., Osborne, C. K., Hilsenbeck, S. G. et al. (2016). Phosphatase PTP4A3 promotes triple-negative breast cancer growth and predicts poor patient survival. *Cancer Res.* **76**, 1942–1953. doi:10.1158/0008-5472.CAN-14-0673
- Dephoure, N., Zhou, C., Villen, J., Beausoleil, S. A., Bakalarski, C. E., Elledge, S. J. and Gygi, S. P. (2008). A quantitative atlas of mitotic phosphorylation. *Proc. Natl. Acad. Sci. USA* **105**, 10762–10767. doi:10.1073/pnas.0805139105
- Dite, T. A., Langendorf, C. G., Hoque, A., Galic, S., Rebello, R. J., Owens, A. J., Lindqvist, L. M., Ngoei, K. R. W., Ling, N. X. Y., Furic, L. et al. (2018). AMP-activated protein kinase selectively inhibited by the type II inhibitor SBI-0206965. *J. Biol. Chem.* **293**, 8874–8885. doi:10.1074/jbc.RA118.003547
- Dobin, A., Davis, C. A., Schlesinger, F., Drenkow, J., Zaleski, C., Jha, S., Batut, P., Chaisson, M. and Gingeras, T. R. (2013). STAR: ultrafast universal RNA-seq aligner. *Bioinformatics* **29**, 15–21. doi:10.1093/bioinformatics/bts635
- Doménech, E., Maestre, C., Esteban-Martínez, L., Partida, D., Pascual, R., Fernández-Miranda, G., Seco, E., Campos-Olivas, R., Pérez, M., Megias, D. et al. (2015). AMPK and PFKFB3 mediate glycolysis and survival in response to mitophagy during mitotic arrest. *Nat. Cell Biol.* **17**, 1304–1316. doi:10.1038/ncb3231
- Domínguez, G., Silva, J., Silva, J. M., García, J. M., Larrondo, F. J., Vargas, J., Sanfrutos, L., Provencio, M., España, P. and Bonilla, F. (2001). Different expression of P14ARF defines two groups of breast carcinomas in terms of TP73 expression and TP53 mutational status. *Genes Chromosomes Cancer* **31**, 99–106. doi:10.1002/gcc.1123
- Dulla, K., Daub, H., Hornberger, R., Nigg, E. A. and Körner, R. (2010). Quantitative site-specific phosphorylation dynamics of human protein kinases during mitotic progression. *Mol. Cell. Proteomics* **9**, 1167–1181. doi:10.1074/mcp.M900335-MCP200
- Fujii, R., Hanamura, T., Suzuki, T., Gohn, T., Shibahara, Y., Niwa, T., Yamaguchi, Y., Ohnuki, K., Kakugawa, Y., Hirakawa, H. et al. (2014). Increased androgen receptor activity and cell proliferation in aromatase inhibitor-resistant breast carcinoma. *J. Steroid Biochem. Mol. Biol.* **144**, 513–522. doi:10.1016/j.jsbmb.2014.08.019
- Guerrero-Martínez, J. A. and Reyes, J. C. (2018). High expression of SMARCA4 or SMARCA2 is frequently associated with an opposite prognosis in cancer. *Sci. Rep.* **8**, 2043. doi:10.1038/s41598-018-20217-3
- Györfi, B., Lanczky, A., Eklund, A. C., Denkert, C., Budczies, J., Li, Q. and Szallasi, Z. (2010). An online survival analysis tool to rapidly assess the effect of 22,277 genes on breast cancer prognosis using microarray data of 1,809 patients. *Breast Cancer Res. Treat.* **123**, 725–731. doi:10.1007/s10549-009-0674-9
- Hirsch, H. A., Iliopoulos, D., Tschlis, P. N. and Struhl, K. (2009). Metformin selectively targets cancer stem cells, and acts together with chemotherapy to block tumor growth and prolong remission. *Cancer Res.* **69**, 7507–7511. doi:10.1158/0008-5472.CAN-09-2994
- Hoffman, L., Jensen, C. C., Yoshigi, M. and Beckerle, M. (2017). Mechanical signals activate p38 MAPK pathway-dependent reinforcement of actin via mechanosensitive HspB1. *Mol. Biol. Cell* **28**, 2661–2675. doi:10.1091/mbc.e17-02-0087
- Inoki, K., Zhu, T. and Guan, K.-L. (2003). TSC2 mediates cellular energy response to control cell growth and survival. *Cell* **115**, 577–590. doi:10.1016/S0092-8674(03)00929-2
- Ito, M., Nakano, T., Erdödi, F. and Hartshorne, D. J. (2004). Myosin phosphatase: structure, regulation and function. *Mol. Cell. Biochem.* **259**, 197–209. doi:10.1023/B:MCBI.0000021373.14288.00
- Kasznicki, J., Sliwinski, A. and Drzewoski, J. (2014). Metformin in cancer prevention and therapy. *Ann. Transl. Med.* **2**, 57. doi:10.3978/j.issn.2305-5839.2014.06.01
- Kops, G. J. P. L., Foltz, D. R. and Cleveland, D. W. (2004). Lethality to human cancer cells through massive chromosome loss by inhibition of the mitotic checkpoint. *Proc. Natl. Acad. Sci. USA* **101**, 8699–8704. doi:10.1073/pnas.0401142101
- Kops, G. J. P. L., Weaver, B. A. A. and Cleveland, D. W. (2005). On the road to cancer: aneuploidy and the mitotic checkpoint. *Nat. Rev. Cancer* **5**, 773–785. doi:10.1038/nrc1714
- Lakshman, M., Subramaniam, V., Rubenthiran, U. and Jothy, S. (2004). CD44 promotes resistance to apoptosis in human colon cancer cells. *Exp. Mol. Pathol.* **77**, 18–25. doi:10.1016/j.yexmp.2004.03.002
- Lara-Gonzalez, P., Westhorpe, F. G. and Taylor, S. S. (2012). The spindle assembly checkpoint. *Curr. Biol.* **22**, R966–R980. doi:10.1016/j.cub.2012.10.006
- Lee, J. H., Koh, H., Kim, M., Kim, Y., Lee, S. Y., Karess, R. E., Lee, S.-H., Shong, M., Kim, J.-M., Kim, J. et al. (2007). Energy-dependent regulation of cell structure by AMP-activated protein kinase. *Nature* **447**, 1017–1020. doi:10.1038/nature05828
- Lee, I. J., Lee, C.-W. and Lee, J.-H. (2015). CaMKK β -AMPK α 2 signaling contributes to mitotic Golgi fragmentation and the G2/M transition in mammalian cells. *Cell Cycle* **14**, 598–611. doi:10.4161/15384101.2014.991557
- Li, B. and Dewey, C. N. (2011). RSEM: accurate transcript quantification from RNA-Seq data with or without a reference genome. *BMC Bioinformatics* **12**, 323. doi:10.1186/1471-2105-12-323
- Liu, B., Fan, Z., Edgerton, S. M., Deng, X.-S., Alimova, I. N., Lind, S. E. and Thor, A. D. (2009). Metformin induces unique biological and molecular responses in triple negative breast cancer cells. *Cell Cycle* **8**, 2031–2040. doi:10.4161/cc.8.13.8814
- Liu, T., Sun, H., Liu, S., Yang, Z., Li, L., Yao, N., Cheng, S., Dong, X., Liang, X., Chen, C. et al. (2018). The suppression of DUSP5 expression correlates with paclitaxel resistance and poor prognosis in basal-like breast cancer. *Int. J. Med. Sci.* **15**, 738–747. doi:10.7150/ijms.24981
- Manchado, E., Guillaumot, M. and Malumbres, M. (2012). Killing cells by targeting mitosis. *Cell Death Differ.* **19**, 369–377. doi:10.1038/cdd.2011.197
- Mao, L., Li, N., Guo, Y., Xu, X., Gao, L., Xu, Y., Zhou, L. and Liu, W. (2013). AMPK phosphorylates GBF1 for mitotic Golgi disassembly. *J. Cell Sci.* **126**, 1498–1505. doi:10.1242/jcs.121954
- Marrone, K. A., Zhou, X., Forde, P. M., Purtell, M., Brahmer, J. R., Hann, C. L., Kelly, R. J., Coleman, B., Gabrielson, E., Rosner, G. L. et al. (2018). A randomized phase II study of metformin plus Paclitaxel/Carboplatin/Bevacizumab in patients with chemotherapy-naïve advanced or metastatic non-small cell lung cancer. *Oncologist* **23**, 859–865. doi:10.1634/theoncologist.2017-0465
- Mihaylova, M. M. and Shaw, R. J. (2011). The AMPK signalling pathway coordinates cell growth, autophagy and metabolism. *Nat. Cell Biol.* **13**, 1016–1023. doi:10.1038/ncb2329
- Mirouse, V., Swick, L. L., Kazgan, N., St Johnston, D. and Brenman, J. E. (2007). LKB1 and AMPK maintain epithelial cell polarity under energetic stress. *J. Cell Biol.* **177**, 387–392. doi:10.1083/jcb.200702053
- Mitchell, K. I., Michell, B. J., House, C. M., Stapleton, D., Dyck, J., Gamble, J., Ullrich, C., Witters, L. A. and Kemp, B. E. (1997). Posttranslational modifications of the 5'-AMP-activated protein kinase beta1 subunit. *J. Biol. Chem.* **272**, 24475–24479. doi:10.1074/jbc.272.39.24475
- Moelans, C. B., Monsuur, H. N., De Pinth, J. H., Radersma, R. D., De Weger, R. A. and Van Diest, P. J. (2011). ESR1 amplification is rare in breast cancer and is associated with high grade and high proliferation: a multiplex ligation-dependent probe amplification study. *Cell. Oncol.* **34**, 489–494. doi:10.1007/s13402-011-0045-5
- Musacchio, A. and Salmon, E. D. (2007). The spindle-assembly checkpoint in space and time. *Nat. Rev. Mol. Cell Biol.* **8**, 379–393. doi:10.1038/nrm2163
- Nakano, A., Kato, H., Watanabe, T., Min, K.-D., Yamazaki, S., Asano, Y., Seguchi, O., Higo, S., Shintani, Y., Asanuma, H. et al. (2010). AMPK controls the speed of microtubule polymerization and directional cell migration through CLIP-170 phosphorylation. *Nat. Cell Biol.* **12**, 583–590. doi:10.1038/ncb2060
- Nam, K. S., Oh, S., Lee, K.-, Yoo, S.- and Shin, I. (2015). CD44 regulates cell proliferation, migration, and invasion via modulation of c-Src transcription in human breast cancer cells. *Cell. Signal.* **27**, 1882–1894. doi:10.1016/j.cellsig.2015.05.002
- Nowak, M. A., Komarova, N. L., Sengupta, A., Jallepalli, P. V., Shih, I.-M., Vogelstein, B. and Lengauer, C. (2002). The role of chromosomal instability in tumor initiation. *Proc. Natl. Acad. Sci. USA* **99**, 16226–16231. doi:10.1073/pnas.202617399
- Oligschlaeger, Y., Miglianico, M., Chanda, D., Scholz, R., Thali, R. F., Tuerk, R., Stapleton, D. I., Gooley, P. R. and Neumann, D. (2015). The recruitment of AMP-activated protein kinase to glycogen is regulated by autophosphorylation. *J. Biol. Chem.* **290**, 11715–11728. doi:10.1074/jbc.M114.633271
- Oliveras-Ferraro, C., Vazquez-Martín, A. and Menéndez, J. A. (2009). Genome-wide inhibitory impact of the AMPK activator metformin on [kinesins, tubulins, histones, auroras and polo-like kinases] M-phase cell cycle genes in human breast cancer cells. *Cell Cycle* **8**, 1633–1636. doi:10.4161/cc.8.10.8406
- Peters, J.-M. (2006). The anaphase promoting complex/cyclosome: a machine designed to destroy. *Nat. Rev. Mol. Cell Biol.* **7**, 644–656. doi:10.1038/nrm1988
- Pino, M. S. and Chung, D. C. (2010). The chromosomal instability pathway in colon cancer. *Gastroenterology* **138**, 2059–2072. doi:10.1053/j.gastro.2009.12.065
- Pinter, K., Jefferson, A., Czibik, G., Watkins, H. and Redwood, C. (2012). Subunit composition of AMPK trimers present in the cytoskeletal apparatus: Implications for drug target identification. *Cell Cycle* **11**, 917–921. doi:10.4161/cc.11.5.19412
- Rao, C. V. and Yamada, H. Y. (2013). Genomic instability and colon carcinogenesis: from the perspective of genes. *Front. Oncol.* **3**, 130. doi:10.3389/fonc.2013.00130
- Reijm, E. A., Jansen, M. P. H. M., Ruigrok-Ritstier, K., Van Staveren, I. L., Look, M. P., Van Gelder, M. E. M., Sieuwerts, A. M., Sleijfer, S., Foekens, J. A. and Berns, E. M. J. J. (2011). Decreased expression of EZH2 is associated with upregulation of ER and favorable outcome to tamoxifen in advanced breast cancer. *Breast Cancer Res. Treat.* **125**, 387–394. doi:10.1007/s10549-010-0836-9
- Reiter, R., Gais, P., Jütting, U., Steuer-Vogt, M. K., Pickhard, A., Bink, K., Rauser, S., Lassmann, S., Höfler, H., Werner, M. et al. (2006). Aurora kinase A messenger RNA overexpression is correlated with tumor progression and shortened survival in head and neck squamous cell carcinoma. *Clin. Cancer Res.* **12**, 5136–5141. doi:10.1158/1078-0432.CCR-05-1650

- Ruiz-Ruiz, C., Munoz-Pinedo, C. and Lopez-Rivas, A. (2000). Interferon-gamma treatment elevates caspase-8 expression and sensitizes human breast tumor cells to a death receptor-induced mitochondria-operated apoptotic program. *Cancer Res.* **60**, 5673–5680.
- Sakuma, T., Nishikawa, A., Kume, S., Chayama, K. and Yamamoto, T. (2014). Multiplex genome engineering in human cells using all-in-one CRISPR/Cas9 vector system. *Sci. Rep.* **4**, 5400. doi:10.1038/srep05400
- Salomon, D. S., Normanno, N., Ciardiello, F., Brandt, R., Shoyab, M. and Todaro, G. J. (1995). The role of amphiregulin in breast cancer. *Breast Cancer Res. Treat.* **33**, 103–114. doi:10.1007/BF00682718
- Sanli, T., Rashid, A., Liu, C., Harding, S., Bristow, R. G., Cutz, J.-C., Singh, G., Wright, J. and Tsakiridis, T. (2010). Ionizing radiation activates AMP-activated kinase (AMPK): a target for radiosensitization of human cancer cells. *Int. J. Radiat. Oncol. Biol. Phys.* **78**, 221–229. doi:10.1016/j.ijrobp.2010.03.005
- Sanli, T., Storozhuk, Y., Linher-Melville, K., Bristow, R. G., Laderout, K., Viollet, B., Wright, J., Singh, G. and Tsakiridis, T. (2012). Ionizing radiation regulates the expression of AMP-activated protein kinase (AMPK) in epithelial cancer cells. *Radiother. Oncol.* **102**, 459–465. doi:10.1016/j.radonc.2011.11.014
- Schvartzman, J.-M., Sotillo, R. and Benezra, R. (2010). Mitotic chromosomal instability and cancer: mouse modelling of the human disease. *Nat. Rev. Cancer* **10**, 102–115. doi:10.1038/nrc2781
- Shichiri, M., Yoshinaga, K., Hisatomi, H., Sugihara, K. and Hirata, Y. (2002). Genetic and epigenetic inactivation of mitotic checkpoint genes hBUB1 and hBUBR1 and their relationship to survival. *Cancer Res.* **62**, 13–17.
- Singh, A. K., Pandey, A., Tewari, M., Kumar, R., Sharma, A., Singh, K. A., Pandey, H. P. and Shukla, H. S. (2013). Advanced stage of breast cancer hoist alkaline phosphatase activity: risk factor for females in India. *3 Biotech* **3**, 517–520. doi:10.1007/s13205-012-0113-1
- Stauffer, S., Chen, X., Zhang, L., Chen, Y. and Dong, J. (2016). KIBRA promotes prostate cancer cell proliferation and motility. *FEBS J.* **283**, 1800–1811. doi:10.1111/febs.13718
- Stauffer, S., Zeng, Y., Zhou, J., Chen, X., Chen, Y. and Dong, J. (2017). CDK1-mediated mitotic phosphorylation of PBK is involved in cytokinesis and inhibits its oncogenic activity. *Cell. Signal.* **39**, 74–83. doi:10.1016/j.cellsig.2017.08.001
- Sun, X., Li, D., Yang, Y., Ren, Y., Li, J., Wang, Z., Dong, B., Liu, M. and Zhou, J. (2012). Microtubule-binding protein CLIP-170 is a mediator of paclitaxel sensitivity. *J. Pathol.* **226**, 666–673. doi:10.1002/path.3026
- Suzuki, T., Bridges, D., Nakada, D., Skiniotis, G., Morrison, S. J., Lin, J. D., Saltiel, A. R. and Inoki, K. (2013). Inhibition of AMPK catabolic action by GSK3. *Mol. Cell* **50**, 407–419. doi:10.1016/j.molcel.2013.03.022
- Thaiparambil, J. T., Eggers, C. M. and Marcus, A. I. (2012). AMPK regulates mitotic spindle orientation through phosphorylation of myosin regulatory light chain. *Mol. Cell. Biol.* **32**, 3203–3217. doi:10.1128/MCB.00418-12
- Tripodi, F., Fraschini, R., Zocchi, M., Reghellin, V. and Coccetti, P. (2018). Snf1/AMPK is involved in the mitotic spindle alignment in *Saccharomyces cerevisiae*. *Sci. Rep.* **8**, 5853. doi:10.1038/s41598-018-24252-y
- Tuazon, P. T. and Traugh, J. A. (1984). Activation of actin-activated ATPase in smooth muscle by phosphorylation of myosin light chain with protease-activated kinase I. *J. Biol. Chem.* **259**, 541–546. doi:10.1111/j.1432-1033.1982.tb07041.x
- Vazquez-Martin, A., Oliveras-Ferreros, C., López-Bonet, E. and Menendez, J. A. (2009). AMPK: Evidence for an energy-sensing cytokinetic tumor suppressor. *Cell Cycle* **8**, 3679–3683. doi:10.4161/cc.8.22.9905
- Vazquez-Martin, A., Oliveras-Ferreros, C., Cufí, S. and Menendez, J. A. (2011). Polo-like kinase 1 regulates activation of AMP-activated protein kinase (AMPK) at the mitotic apparatus. *Cell Cycle* **10**, 1295–1302. doi:10.4161/cc.10.8.15342
- Vazquez-Martin, A., Cufí, S., Oliveras-Ferreros, C. and Menendez, J. A. (2012). Polo-like kinase 1 directs the AMPK-mediated activation of myosin regulatory light chain at the cytokinetic cleavage furrow independently of energy balance. *Cell Cycle* **11**, 2422–2426. doi:10.4161/cc.20438
- Vitale, I., Galluzzi, L., Castedo, M. and Kroemer, G. (2011). Mitotic catastrophe: a mechanism for avoiding genomic instability. *Nat. Rev. Mol. Cell Biol.* **12**, 385–392. doi:10.1038/nrm3115
- Wei, C., Bhattaram, V. K., Igwe, J. C., Fleming, E. and Tirnauer, J. S. (2012). The LKB1 tumor suppressor controls spindle orientation and localization of activated AMPK in mitotic epithelial cells. *PLoS ONE* **7**, e41118. doi:10.1371/journal.pone.0041118
- Woods, A., Vertommen, D., Neumann, D., Türk, R., Bayliss, J., Schlattner, U., Wallimann, T., Carling, D. and Rider, M. H. (2003). Identification of phosphorylation sites in AMP-activated protein kinase (AMPK) for upstream AMPK kinases and study of their roles by site-directed mutagenesis. *J. Biol. Chem.* **278**, 28434–28442. doi:10.1074/jbc.M303946200
- Xiao, L., Chen, Y., Ji, M. and Dong, J. (2011). KIBRA regulates Hippo signaling activity via interactions with large tumor suppressor kinases. *J. Biol. Chem.* **286**, 7788–7796. doi:10.1074/jbc.M110.173468
- Zadra, G., Batista, J. L. and Loda, M. (2015). Dissecting the dual role of AMPK in cancer: from experimental to human studies. *Mol. Cancer Res.* **13**, 1059–1072. doi:10.1158/1541-7786.MCR-15-0068
- Zakikhani, M., Dowling, R., Fantus, I. G., Sonenberg, N. and Pollak, M. (2006). Metformin is an AMP kinase-dependent growth inhibitor for breast cancer cells. *Cancer Res.* **66**, 10269–10273. doi:10.1158/0008-5472.CAN-06-1500
- Zeng, Y., Stauffer, S., Zhou, J., Chen, X., Chen, Y. and Dong, J. (2017). Cyclin-dependent kinase 1 (CDK1)-mediated mitotic phosphorylation of the transcriptional co-repressor Vgll4 inhibits its tumor-suppressing activity. *J. Biol. Chem.* **292**, 15028–15038. doi:10.1074/jbc.M117.796284
- Zhang, L., Chen, X., Stauffer, S., Yang, S., Chen, Y. and Dong, J. (2015). CDK1 phosphorylation of TAZ in mitosis inhibits its oncogenic activity. *Oncotarget* **6**, 31399–31412. doi:10.18632/oncotarget.5189
- Zhou, J., Zeng, Y., Cui, L., Chen, X., Stauffer, S., Wang, Z., Yu, F., Lele, S. M., Talmon, G. A., Black, A. R. et al. (2018). Zyxin promotes colon cancer tumorigenesis in a mitotic phosphorylation-dependent manner and through CDK8-mediated YAP activation. *Proc. Natl. Acad. Sci. USA* **115**, E6760–E6769. doi:10.1073/pnas.1800621115

Table S1

AMPK guide sequences

<u>Oligo name</u>	<u>Sequence</u>
PRKAB1-A-Fwd	caccGCAGCGCGGCGCGCTCACTGC
PRKAB1-A-Rev	aaacGCAGTGAGCGCGCCGCGCTGC
PRKAB1-B-Fwd	caccGTGGCCATAAGACGCCCCGG
PRKAB1-B-Rev	aaacCCGGGGCGTCTTATGGCCAC
PRKAA1-A-Fwd	caccGGCTGTCGCCATCTTTCTCC
PRKAA1-A-Rev	aaacGGAGAAAGATGGCGACAGCC
PRKAA1-B-Fwd	caccGAAGATCGGCCACTACATTC
PRKAA1-B-Rev	aaacGAATGTAGTGGCCGATCTTC
PRKAA2-A-Fwd	caccGTCAGCCATCTTCGGCGCGCG
PRKAA2-A-Rev	aaacCGCGCGCCGAAGATGGCTGAC
PRKAA2-B-Fwd	caccGAAGATCGGACACTACGTGC
PRKAA2-B-Rev	aaacGCACGTAGTGTCCGATCTTC

Fwd: forward; Rev: reverse

Supplemental Figure 1

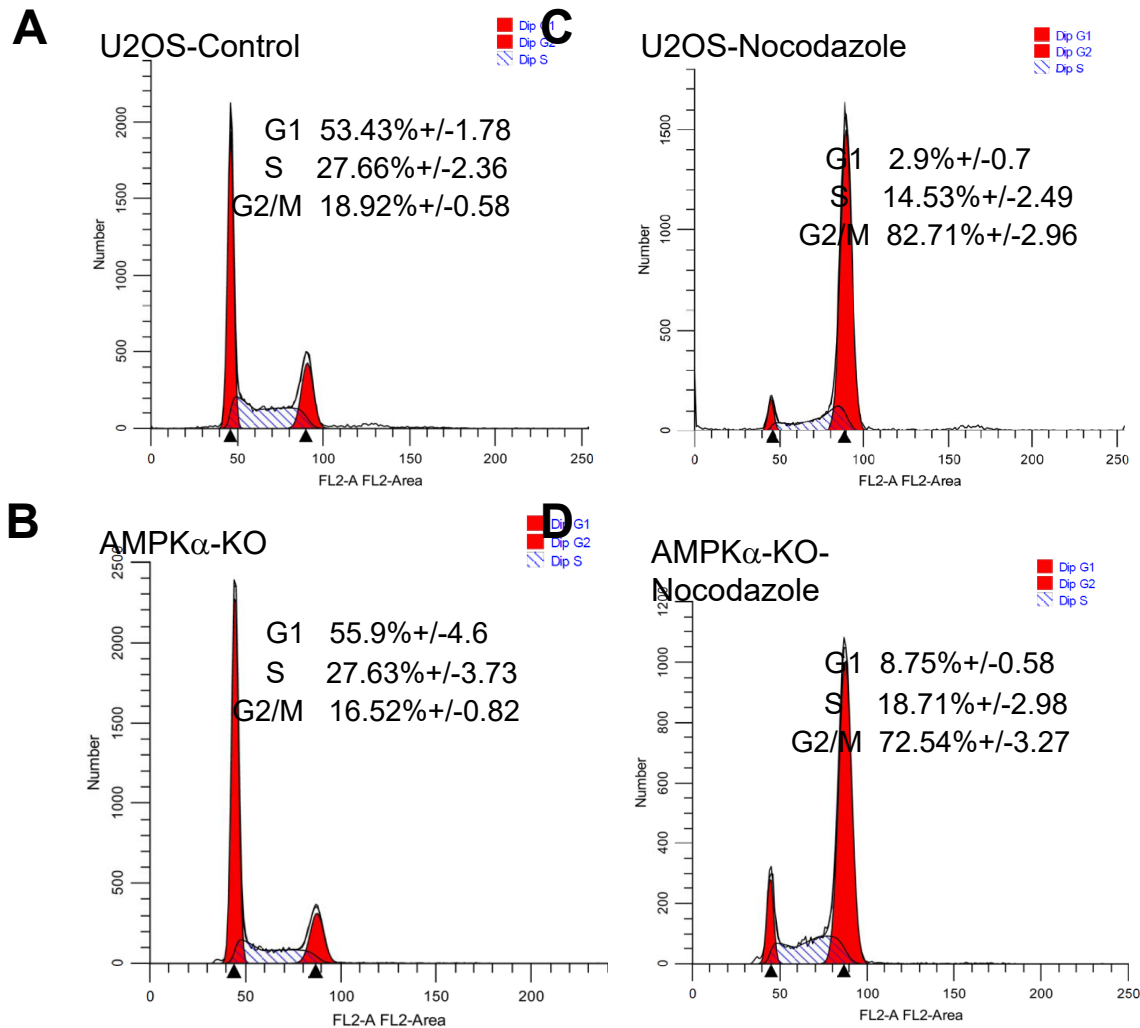


Fig. S1 FACS analysis of control and AMPK α -KO cells. Cells were treated with DMSO (control) (A, B) or Nocodazole (100 ng/mL for 20 h) (C, D) and cells were then stained by PI analyzed by flow cytometry. Numbers for each cell cycle phases are from three repeats.